Performance Evaluation of Full Adder Using Mach–Zehnder Interferometer and Polarization Effect on WDM Channels

A thesis submitted in partial fulfillment of the requirements for the award of degree of

Master of Engineering
in
Electronics & Communication Engineering

Submitted by
Neeraj Maurya
Reg. No- 80761016

Under the esteemed guidance of
Ms. Smarti Reel
Lecturer ECED
Thapar University, Patiala

Department of Electronics and Communication Engineering
Thapar University
Patiala-147004, India
June-2009

CERTIFICATE

I hereby certify that the work which is being presented in this thesis entitled, **"Performance Evaluation of Full Adder Using Mach–Zehnder Interferometer and Polarization Effect on WDM Channels,"** in partial fulfillment of the requirements for the award of degree of **Master of Engineering** in **Electronics & Communication Engineering Department** at **Thapar University, Patiala,** is an authentic record of my own work carried out under the supervision of **Ms. Smarti Reel** and refers other researcher's work which are duly listed in the reference section.

The matter embodied in this thesis has not been submitted for the award of any other degree to any other university.

Date: 15-07-09

Neeraj Maurya
(Reg. No. 80761016)

This is to certify that the above statement made by the candidate is correct and true to best of my knowledge.

Ms. Smarti Reel
Lecturer, ECED
Thapar University,
Patiala-147004

Counter signed by

23.7.09

Dr. A. K. Chatterjee
Professor & Head,
Electronics & Communication Engg. Department
Thapar University,
Patiala-147004

24/7

Dr. R. K. Sharma
Dean of Academic Affairs
Thapar University,
Patiala-147004

ACKNOWLEDGEMENT

Words are often too less to reveal one's deep regards. An understanding of the work like this is never the outcome of the efforts of a single person. I take this opportunity to express my profound sense of gratitude and respect to all those who helped me through the duration of this thesis.

First of all I would like to thank the **Supreme Power,** one who has always guided me to work on the right path of the life. Without his grace this would never come to be today's reality.

This work would not have been possible without the encouragement and able guidance of my supervisor, **Ms. Smarti Reel.** Her enthusiasm and optimism made this experience both rewarding and enjoyable. Most of the novel ideas and solutions found in this thesis are the result of our numerous stimulating discussions. Her feedback and editorial comments were also invaluable for the writing of this thesis.

No words of thanks are enough for my **dear parents** whose support and care makes me stay on earth. Thanks to be with me.

At the end, I would like to thank all the faculty members of the department and my all friends especially directly or indirectly helped me in completion of my thesis.

NEERAJ MAURYA

Abstract

The optical communication system has many advantages over the long distance communication and fast switching. The requirements of data transmission for communication are increasing day by day. But the bandwidth is limited for transmission. In this thesis, two types of techniques are discussed for transmitting the data from transmitter to receiver.

Firstly Mach–Zehnder Interferometric devices for optical processing which is used as a wavelength-spacing tunable comb filter in a fiber ring laser is built by employing an optical variable delay line (OVDL). Semiconductor optical amplifier (SOA)-based Mach–Zehnder interferometer (MZI) and Optical tree architecture (OTA), both play an important role in optical interconnecting networks. In this thesis the proposed SOA-MZI-based tree architecture is used with new and alternative scheme, for integrated all-optical logic and arithmetic operations. In this architecture the continuous wave laser source and control signal are passes through the coupler. The pulsed signal at the wavelength λ_1 is split at coupler and more power passes through one arm. At the same time, the CW signal at wavelength λ_2 is split equally by this coupler and propagates simultaneously in the two arms. This architecture can enable to perform all-optical processing of signals, like half-adder, full-adder, etc.

Secondly in optical communication data can be transmitting into the fiber by different techniques. In the proposed architecture the data is send by wave division multiplexing techniques from transmitting end and the effect of polarization seen on channel spacing is 50 GHz and they are generated in groups by odd and even channels by PRBS generator. Initially all channels have the same polarization state. All even channels before being multiplexed with odd channels are passed through the Polarization Shifter, which rotates the polarization state by different angle. After multiplexing the signal is launched into a fiber, and then is de-multiplexed and sent to 8 receivers. At the receiving end measured BER is minimum and Q-factor is maximum for 90 degree state of polarization.

CONTENTS

LIST OF FIGURES

List of Tables

LIST OF ABBREVIATIONS

BER	Bit error rate
CPM	Cross Polarization Modulation
CWLS	Continuous Wave Laser Source
FWM	Four Wave Mixing
MIMD	Multiple Instruction Multiple Data
MZI	Mach–Zehnder interferometers
NOLM	Nonlinear Optical Loop Mirror
OTA	Optical Tree Architecture
OTDM	Optical Time Division Multiplexing
PDG	Polarization Dependent Gain
PLC	Planer Light Wave Circuit
PPLN	Periodically Poled Lithium Niobate
PRBS	Pseudo Random Bit Sequence
SMZ	Symmetric Mach–Zehnder
SOAs	Semiconductor Optical Amplifiers
TOAD	Terahertz optical Asymmetric De-multiplexers
UNI	ultra-fast nonlinear interferometers
VCSEL	Vertical-Cavity Surface-Emitting Lasers
VCSOA	Vertical Cavity Semiconductor Optical Amplifiers
WDM	Wavelength Division Multiplexing
XGM	Cross Gain Modulation
XPM	Cross Phase Modulation

Chapter1

INTRODUCTION

1.1 Introduction

Due to increasing demand of data transfer and high-Speed optical telecommunication networks with terabit transmission capabilities can be achieved if the data remain in the optical format and bottlenecks due to the optical to electronic conversion are avoided. Recently, 5.12- and 3-Tb/s transmission by combined OTDM and WDM (128 40 Gb/s, 19 160 Gb/s) has been successfully demonstrated [1], [2]. These systems require ultrafast signal processing like optical multiplexing add/drop functions, and wavelength conversion. Nonlinear optical loop mirrors (NOLMs) where the switching mechanism is based on fiber Kerr nonlinearities have been used to de-multiplex single-wavelength data rates up to 640 Gb/s [3]. However, due to the weak Kerr coefficient in fibers, long fibers and high optical powers are necessary. More efficient and compact solutions can be realized by all-optical switching in semiconductor optical amplifiers (SOAs) where the nonlinear coefficient is much higher. Various SOA-based switching configurations have been demonstrated, such as terahertz optical asymmetric de-multiplexers [(TOADs) [4], ultrafast nonlinear interferometers [(UNIs) [5], [6]], and Mach–Zehnder interferometers [(MZIs) [7]–[10]]. Among different topologies, monolithically integrated MZI switches represent the most promising solution due to their compact size, thermal stability, and low-power operation. MZI switches have demonstrated single-channel OTDM at up to 168 Gb/s and might even be used for higher data rates [7], [8]. Considering various MZI configurations, the symmetric MZI structure provides the highest flexibility and shortest switching windows [9]. In this switch, two SOAs, one in each arm of the interferometer, are excited by short control pulses with an appropriate time delay. This particular switching mechanism cancels out the slow carrier relaxation (several hundreds of ps) leading to nearly ideal switching windows [12]. However, repetition rates higher than 500 Gb/s require subpicosecond signal pulse widths and the switching windows must approach the picoseconds limit. In terabit per second (Tb/s) applications, signal and control pulses even have subpicosecond pulse delays and partial pulse overlaps will be

difficult to avoid. Therefore, subpicosecond nonlinearities become of prime importance considerably influencing the switching performance [13].

The demand for faster optical communication networks has been on the rise in recent years. To accommodate this demand, the new generation of optical communication networks is moving towards terabit per second data rates. Such data rates can be achieved if the data remain in the optical domain eliminating the need to convert the optical signals to electronic signals and back to optical signals [14]. Therefore, to successfully be able to achieve higher data rates, advanced optical networks will require all optical ultra- fast signals processing such as wavelength conversion, optical logic and arithmetic processing, add–drop function, etc. Various architectures, algorithms, logical and arithmetic operations have been proposed in the field of optical/optoelectronic computing and parallel processing in the last three decades. The silica- on-silicon technology has also been used to make a compact MZ de-multiplexer in a symmetric configuration that was capable of de-multiplexing a 168-Gb/s signal [15]. In almost all the above cases, a single port (cross port) is used to take the output signal. But the signal that exits from the other port (bar port) remains unused. In this communication tried to utilize the output of both the ports of the device. That is, light coming out from the cross port and bar port is taken into account. The light signal that exits through the bar port and also from the cross port of an SOA- based MZI switch is used to design an optical tree-net architecture. In digital optical computing, optical interconnecting systems are the primitives that constitute various optical algorithms and architectures. Optical tree architecture (OTA) also takes an important role in this regard [16,17]. In this communication proposed a new and alternative scheme, which exploits the advantages of both SOA-MZI and OTA, for implementation of all-optical parallel logic and arithmetic operations (half adder, full-adder and full-subtractor) of binary data. In this thesis also tried to exploit the inherent advantages of OTA for designing an all-optical digital data comparison scheme. Here, propose a one-bit binary comparison scheme that can compare any two- bit, i.e. between 0 and 0, 0 and 1, 1 and 0, and 1 and 1. The possibilities of its practical implementation of the proposed scheme are also discussed.

1.2 Semiconductor Optical Amplifier Based MZI Switch

Semiconductor optical amplifiers are amplifiers which use a semiconductor to provide the gain medium. These amplifiers have a similar structure to Fabry-Perot laser diodes but

with anti-reflection design elements at the end faces. Recent designs include anti-reflective coatings and tilted waveguide and window regions which can reduce end face reflection to less than 0.001%. Since this creates a loss of power from the cavity which is greater than the gain it prevents the amplifier from acting as a laser. This type of amplifiers are often used in telecommunication systems in the form of fibre-pigtailed components, operating at signal wavelengths between 0.85 μm and 1.6 μm and generating gains of up to 30 dB.

The semiconductor optical amplifier is of small size and electrically pumped. It can be potentially less expensive than the EDFA and can be integrated with semiconductor lasers, modulators, etc. However, the performance is still not comparable with the EDFA. The SOA has higher noise, lower gain, moderate polarization dependence and high nonlinearity with fast transient time. This originates from the short nanosecond or less upper state lifetime, so that the gain reacts rapidly to changes of pump or signal power and the changes of gain also cause phase changes which can distort the signals.

This nonlinearity presents the most severe problem for optical communication applications. However it provides the possibility for gain in different wavelength regions from the EDFA. "Linear optical amplifiers" using gain-clamping techniques have been developed.

An MZI switch, as shown in Fig.1.1 is a very powerful technique to realize ultra-fast switching. In this switch a SOA is inserted in each arm of an MZI [15]. The pulsed signal at the wavelength $\lambda 1$ is split at the first coupler such that more power passes through one arm. At the same time, the CW signal at the wavelength $\lambda 2$ is split equally by this coupler and propagates simultaneously in the two arms. In the absence of the $\lambda 1$ beam, the CW beam exits from the cross port (lower port in the figure). However, when both beams are present simultaneously, all one bits are directed towards the bar port (upper port in the figure) because of the refractive-index change induced by the $\lambda 1$ beam. The physical mechanism behind the behaviour is cross-phase modulation (XPM). Gain saturation induced by the $\lambda 1$ beam reduces carrier density inside one SOA, which in turn increases the refractive index only in the arm through which the $\lambda 1$ beam passes.

As a result, an additional phase shift can be introduced on the CW beam because of

XPM, and the CW wave is directed towards the bar port during each one bit. Optical filters are placed in front of the output ports for blocking the original λ_1 signal. The MZ scheme is preferable over cross-gain saturation as it does not reverse the bit pattern and results in a higher on–off contrast simply because nothing exits from the bar port during 0 bits [15].

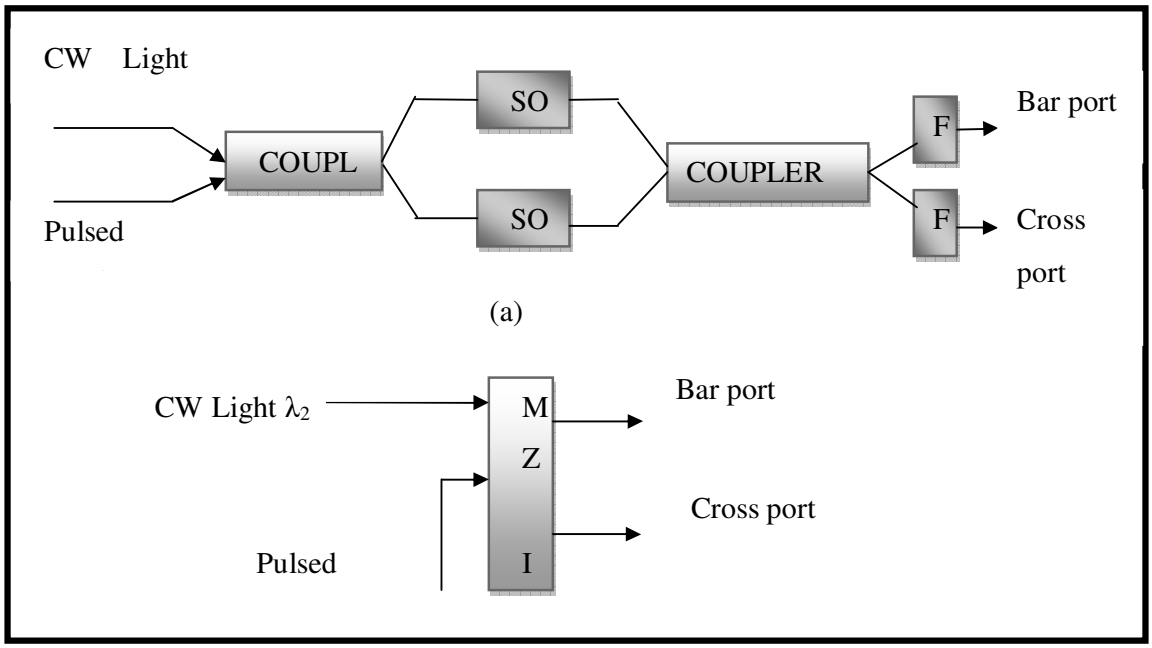

Fig.1.1 (a) SOA-based MZI optical switch. (b) Schematic diagram of SOA-based MZI optical switch.

Now, it is clear that in the absence of control signal (λ **1**), the incoming signal (CW signal) exits through the cross port (lower channel) of MZI as shown in Fig. 1(a). In this case no light is present in the bar port (upper channel). But in the presence of control signal, the incoming signal exits through the bar port of the MZI as shown in Fig.1.1 (a). In this case no light is present in the cross port. In the absence of incoming signal, the bar- port and cross port receive no light as the filter blocks the control signal. A schematic block diagram is shown in Fig.1.1 (b). In our present proposal, the above characteristics of an MZI are utilized for designing a tree-net architecture in all-optical domain, which can successfully be exploited for all-optical logic and arithmetic operations (half-adder, half-sub-tractor, full-adder, full-sub-tractor, data comparator).

1.3 Optical Tree Architecture

Optical tree architecture is a multiplying system of single straight path into several distributed branches and sub- branch paths [16]. This structure is explained in Fig.1.2. Here a light beam coming through a single path and distributed at point N into two parts NO and NP. These two beams again distributed into four parts, i.e. NO to OQ and OR, and NP to PS and PT. In this way, there are number of output channels could be obtained from a single input light beam.

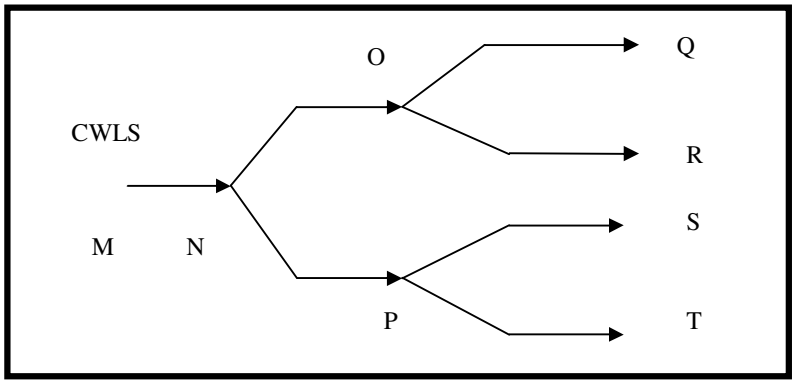

Fig.1.2 Optical tree architecture

If the situation requires more spatially distributed output channels or terminals, another splitting arrangement is to be inserted in the last output channels.

1.4 Tree Architecture with MZI Optical Switch

An SOA based MZI switching system, discussed in Section2, can successfully be used for the designing of OTA. For this purpose, three MZI optical switches s1, s2 and s3 are to be set at N, O and P, respectively. These switches control the light in such a manner that, in the absence of control signal, the incoming light signal emerges from the lower channel of the switch. In the presence of control signal, the incoming signal emerges from the upper channel. Now, let us consider that there is constant source of CW beam (of wavelength $\lambda 1$), CWLS, which may be a laser source. The light signal that comes from CWLS can be taken as the incoming signal. The incoming light signal is incident on switch s1 first. The light could be taken from different desired branches or sub-branches by the proper placing of control signals. Control signals are also the light signals. The schematic diagram is shown in Fig. 1.3.

Here the two control signals A and B. They can take two binary values 1 or 0. The presence of light beam is considered to be as one (1) state and the absence of light beam as zero (0) state. Hence, the control A and B in four ways (A =0, B =0; A = 0, B = 1; A = 1, B = 0; A = 1, B = 1). Here explain the working principle of optical tree using MZI-based optical switches as shown in Fig.1.3 in detail.

Case 1: When A = 0 and B = 0

In this type of optical switch the CW light beam that comes from constant CWLS is incident on switch s1 first. As here A = 0, the control signal A is absent. That means that only incoming light signal is present at s1. As per the switching principle, discussed above, the light emerges through the lower channel and falls on switch s3 at P. Here the control signal B is also absent. That means here also only incoming light signal is present at s3. Hence, the light finally comes out through lower channel of s3 and reaches T-1 (terminal-1). In this case, no light is present at other terminals T-2 (terminal-2), T-3 (terminal-3) and T-4 (terminal-4). So T-1 is in one state and the others are in zero state, when A = B = 0.

Case 2: When A = 0 and B = 1

Light from the CW light source is incident on s1. As A = 0, the light beam emerges through the lower channel and falls on s3. At s3, the control signal B is present. In the presence of the control signal, the incoming light signal emerges through the upper channel of s3 and finally reaches T-2. In this case light is only present in T-2. Hence T-2 is in one state and the others are in zero state, when A = 0 and B = 1.

Case 3: When A = 1 and B = 0

Light from the CW light source is incident on s1. As A = 1, the control signal A is present. Because of that, light beam emerges through the upper channel of s1 and falls on s2 at O. As B=0, no control signal is present at B, That means the light comes out from the lower channel of s2 to reachT-3. SoT-3 is in one state and the others are in zero state, when A = 1 and B = 0.

Case 4: When A = 1 and B = 1

The light from CWLS is incident on switch s1 first. As here A = 1, the input control signal A is present. Because of that, the light emerges through the upper channel of s1 and falls on s2 at O. As B = 1, the control signal is present at B. Hence, the light follows the upper channel of s2 to reachT-4. SoT-4 is in one state and the others are in zero state, when A = 1 and B = 1.

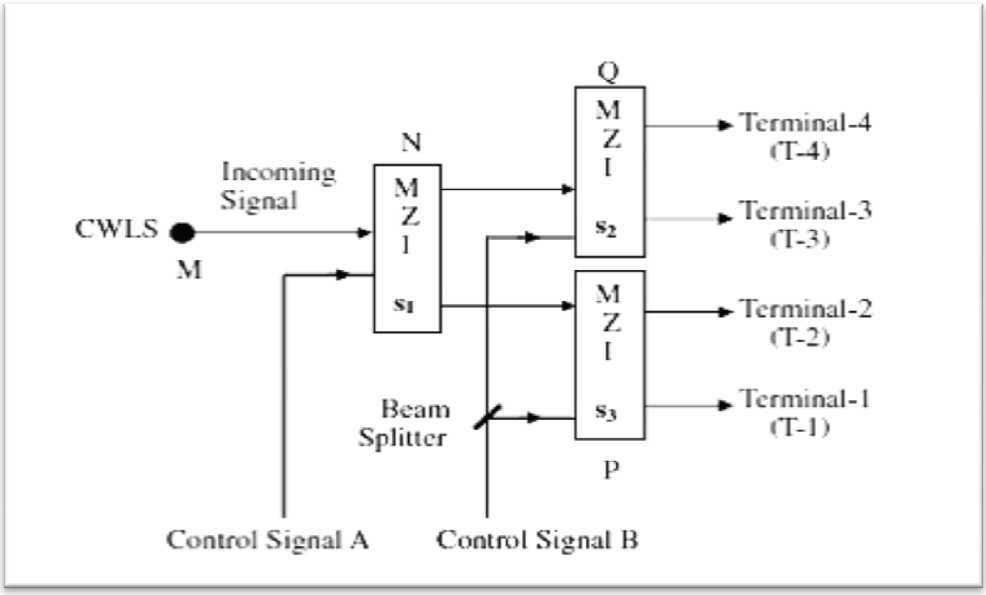

Fig.1.3 MZI optical switch in tree architecture [18]

Table 1.1 State of different output terminals for different values of A and B in tree architecture

Input		Output At Different Terminal			
A	B	Terminal-1	Terminal-2	Terminal-3	Terminal-4
0	0	1	0	0	0
0	1	0	1	0	0
1	0	0	0	1	0
1	1	0	0	0	1

In the information age, the relentless demand for networks of higher capacities at lower costs. Optical communication technology has developed rapidly to achieve larger transmission capacity and longer transmission distance. For that such data rates can be

achieved if the data remain in the optical domain eliminating the need to convert the optical signals. Therefore, to successfully be able to achieve higher data rates, advanced optical networks will require all optical ultra fast signal processing such as wavelength conversion, optical logic and arithmetic processing, add-drop function, etc. Various architectures, algorithms, logical and arithmetic operations have been proposed in the field of optical/optoelectronic computing and parallel processing in the last three decades. Nonlinear optical loop mirror (NOLM) provides a major support to optical switching based all optical logic and algebraic processing where the switching mechanism is based on fiber Kerr nonlinearities. More efficient and compact solutions can be realized by all optical switching in semiconductor optical amplifiers (SOAs) where the non linear coefficient is much higher. Various SOA based switching configurations have been demonstrated earlier such as Terahertz optical asymmetric demultiplexers (TOADs), ultra-fast nonlinear interferometers (UNIs) and Mach-Zehnder interferometers (MZIs). Among different topologies, monolithically integrated MZI switches represent the most promising solution due to their compact size, thermal stability and low power. In optical computing, optical interconnecting systems are the primitives that constitute various optical algorithms and architectures. Optical tree architecture (OTA) also takes an important role in this regard. So in this era of rapidly changing technology that represent a new alternative scheme which exploits advantages of both SOA-MZI and OTA, for implementation of all optical parallel logic and arithmetic operations of binary data. [4].

1.5 Mach Zehnder Interferometer

The Mach-Zehnder Interferometer is a device used to determine the phase shift caused by a small sample which is placed in the path of one of two collimated beams from a coherent light source. A Mach-Zehnder Interferometer is created from two couplers connected by arms of unequal optical length. The Mach-Zehnder Interferometer has two input ports and two output ports. The light is split in the two arms of the input coupler of the interferometer, and they are later recombined in the output coupler of the interferometer. The optical length of the two arms is unequal, making the phase corresponding to delay in Fig.1.4 to be a function of wavelength. The relative phase of the light in the two input ports of the output coupler is therefore a function of wavelength. As the phase of the delay (d) is increased, the MZI cycles between the cross state, where most of the light appears in the waveguide on the same side as the input, and the bar state,

where most the light moves to the waveguide on the other side. Extensive research has been carried out over the years in developing practical optical time division multiplexing (OTDM) systems considering its vast potential in future high-speed photonic networks.

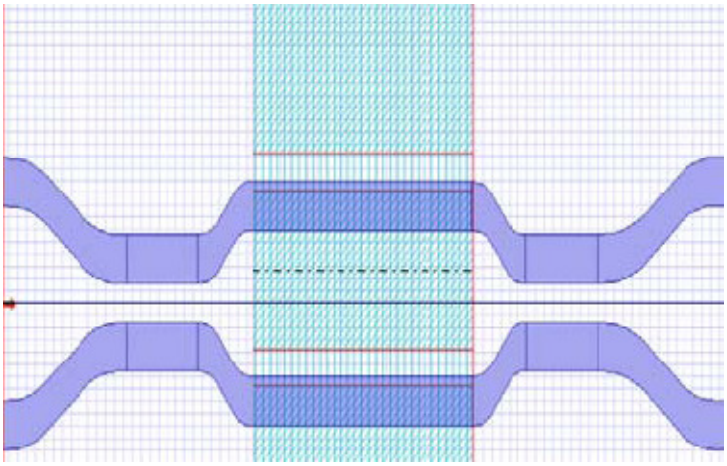

Fig 1.4 Diagram of MZ Interferometer

They have used periodically poled lithium niobate (PPLN) hybrid integrated with planer light wave circuit (PLC) for multiplexing of different channels and studied an all channel multiplexer (MUX) and de-multiplexer (DEMUX) systems. Important characteristics of optical switches include extinction ratio, insertion loss, crosstalk, and switching time. The performance of optical switches is compared on basis of these parameters. Important characteristics of optical switches include extinction ratio, insertion loss, crosstalk, and switching time. The performance of optical switches is compared on basis of these parameters. Investigations revealed that among all the switches symmetric Mach–Zehnder (SMZ) were found to be most suitable because of compact size, thermal stability, and low power operation analysis [6]. It was also outlined that SMZ has symmetric switching window and hence it is less venerable to jitter. The main advantage of SMZ structure over other interferometric switches like terahertz optical asymmetric de-multiplexer (TOAD) is that SMZ can be easily integrated on to a single photonic chip. It is important to mention that OTDM is a time synchronized system and proper signal recovery cannot be achieved without synchronization between the transmitter and the receiver. Inclusion of optical fiber would involve a time delay incurred due to propagation of the signal over the fiber. So the proposed a idea of OTDM system using SMZ switching as this system involves an all channel independent MUX propagation on a fiber of given length and all channel DEMUX.[7,8]

1.6 Optical Switch Fabrics

In the effort to extend optics from transmission to switching, all-optical switching fabrics lay a central role. These devices allow switching directly in all optical domains, avoiding the need for several O/E/O conversions. Given the wide range of possible applications for these devices, it seems reasonable to foresee that there will not be a single winning solution. In briefly enlist the parameters that are taken into account while evaluating an optical switch. The most important parameter of a switch is the switching time. Different applications have different switching time requirements. Other important parameters of a switch can be summarized as follows:

1.6.1 Insertion loss

This is defined as the fraction of signal power that is lost because of the switch. This loss is usually measured in decibels and must be as small as possible. In addition, the insertion loss of a switch should be almost same for all input–output connections (loss uniformity)

1.6.2 Crosstalk

It refers to any phenomenon by which a signal transmitted on one circuit or channel of a transmission system creates an undesired effect in another circuit or channel. Crosstalk is usually caused by undesired capacitive, inductive, or conductive coupling from one circuit, part of a circuit, or channel to another. This is the ratio of the power at a specific output from the desired input to the power from all other inputs.

1.6.3 Extinction ratio (ON–OFF switches)

This is the ratio of the output power in the on-state of the switch to the output power in the off-state. This ratio should be as large as possible. In telecommunications, extinction ratio (*r*e) is the ratio of two optical power levels, of a digital signal generated by an optical source, *e.g.,* a laser diode, where *P* 1 is the optical power level generated when the light source is "on" and *P* 2 is the power level generated when the light source is "off" [re= P1 / P2]. The extinction ratio may be expressed as a fraction or in dB. Extinction ratio measurement can be done on an eye diagram also.

1.6.4 Polarization dependent loss (PDL)

If the loss of the switch is not equal for both states of polarization of the optical signal, the switch is said to have polarization-dependent losses. Polarization dependent loss is a measure of the peak-to- peak difference in transmission of an optical component or system with respect to all possible states of polarization. It is the ratio of the maximum and the minimum transmission of an optical device with respect to all polarization states. It is desirable that optical switches have low PDL. Other parameters that are taken into account include reliability, energy usage, scalability, and temperature resistance. The term scalability refers to the ability to build switches with large port counts that perform adequately. It is particularly an important concern. Many waveguide modulators or switches employ metallic electrodes deposited on top of optical waveguides to serve the purpose of applying the electric field. By means of an external applied voltage, a change in the index of refraction of an optical medium is produced. This produces a bending effect on light transmitted through the medium. Variation in the applied voltage can be used to vary the refractive index or a refractive index gradient may be produced by providing a gradient in the applied field, so as to produce no moving parts scanning of the optical beam. An intermediate buffer layer with a low dielectric constant is often deposited between the electrodes and the substrate to reduce the losses that are due to the metallic cover of the waveguide. By changing electrode parameters could be optimize the device. Usually the electrode in electro optic devices is plated to a thickness of 2-3 microns in order to reduce its ohmic losses while the electrode width can be as small as 10 microns and the gap between electrodes is typically 5 microns. From the electro-optic perspective LiNbO3 is a tri-diagonal crystal with the point group symmetry 3m. The matrix of the electro-optic or pockel's coefficients for the group 3m crystals is [19] This paper is oriented towards the design of an electro optic 2x2 switch based on integrated Mach-Zehnder interferometer. An electro optic switch is a device used in integrated fibre optics. It is capable of changing its state in a very small time, typically in less than a nanosecond. This switching time limit is determined by the capacitance of the electrode configuration. Electro-optic switches are reliable but at the cost of higher driving voltage which in turn limits the switching speed. Larger switches can be realized by integrating several 2x2 switches on a single substrate. However they tend to have a relatively high loss and polarization dependent losses and are more expensive than mechanical switches. The proposed device is based on Mach-Zehnder interferometer made by Titanium

diffusion in Lithium Niobate substrate. MZI can also use magnesium diffusion in Lithium Niobate substrate. The switching between the ports is achieved by an electro optic effect within such structure. Voltage applied to the electrodes deposited on the integrated Mach-Zehnder interferometer, creates an electric field distribution within the substrate, which consequently changes its refractive index. If properly designed, the induced change in the refractive index leads to different coupling between individual ports. The design steps include CAD design of the circuit layout, definition of an input field and simulation run. Usually, there is a trade-off between different aspects of switch design. The most popular architectures for building large switches are the crossbar.

(a) Crossbar:

An n x n crossbar is made of 2x2 switches. The interconnection between the inputs and the outputs is achieved by appropriately setting the states of the n 2x2 switches. The connection rule that is used states that to connect input to output, the path taken traverses the 2x2 switches in row until it reaches column and then traverses the switches in column until it reaches output. The crossbar architecture is wide-sense non-blocking; therefore, as long as the connection rule mentioned previously is used. The shortest path length is 1, and the longest path length is 2n-1, and this is one of the main drawbacks of the crossbar architecture. The switch can be fabricated without any crossovers.

(b) Benes

The Benes architecture is rearrange- ably non blocking switch architecture and is one of the most efficient switch architectures in terms of the number of 2x2 switches it uses to build larger switches. An nxn Benes switch requires (n/2) (2log2n -1) 2x2 switches, being a power of 2. The loss is the same through every path in the switch each path goes through (2logn -1) 2x2 switches. Its two main drawbacks are that it is not wide-sense non-blocking and that a number of waveguide crossovers are required, making it difficult to fabricate in integrated optics.

(c) Spanke–Benes (Stage Planar Architecture)

This switch architecture is a good compromise between the crossbar and Benes switch architecture. It is rearrange ably non-blocking and requires n (n-1)/2 switches. The shortest path length is n/2, and the longest path length is *n*. There are no crossovers. Its main drawbacks are that it is not wide-sense non-blocking and that the loss is not uniform.

(d)Spanke

This architecture is suitable for building large non-integrated switches. A switch is made by combining 1xn switches, along with n nx1 switches. The architecture is strict sense non-blocking and requires 2n(n-1) 1x2 switches, and each path has length 2log2n

1.7 Semiconductor Optical Amplifier

Semiconductor optical amplifiers are amplifiers which use a semiconductor to provide the gain medium. Recent designs include anti-reflective coatings and tilted waveguide and window regions which can reduce end face reflection to less than 0.001%. Since this creates a loss of power from the cavity which is greater than the gain it prevents the amplifier from acting as a laser. Such amplifiers are often used in telecommunication systems in the form of fiber pigtailed components, operating at signal wavelengths between 0.85 μm and 1.6 μm and generating gains of up to 30 dB. The semiconductor optical amplifier is of small size and electrically pumped. It can be potentially less expensive than the EDFA and can be integrated with semiconductor lasers, modulators, etc. However, the performance is still not comparable with the EDFA. The SOA has higher noise, lower gain, moderate polarization dependence and high nonlinearity with fast transient time. This originates from the short nanosecond or less upper state lifetime, so that the gain reacts rapidly to changes of pump or signal power and the changes of gain also because phase changes which can distort the signals. This nonlinearity presents the most severe problem for optical communication applications. However it provides the possibility for gain in different wavelength regions form the EDFA [11].

1.7.1Vertical-cavity SOA

A recent addition to the SOA family is the vertical-cavity SOA (VCSOA). These devices are similar in structure to, and share many features with, vertical-cavity surface-emitting lasers (VCSELs). The major difference when comparing VCSOAs and VCSELs is the reduced mirror reflectivities used in the amplifier cavity. With VCSOAs, reduced feedback is necessary to prevent the device from reaching lasing threshold. Due to the extremely short cavity length, and correspondingly thin gain medium, these devices exhibit very low single-pass gain (typically on the order of a few percent) and also a very large free spectral range (FSR). The small single-pass gain requires relatively high mirror reflectivities to boost the total signal gain. In addition to boosting the total signal gain, the

use of the [[resonant cavity]] structure results in a very narrow gain bandwidth; coupled with the large FSR of the optical cavity, this effectively limits operation of the VCSOA to single-channel amplification. Thus, VCSOAs can be seen as amplifying filters.

1.8 Categories of Switch

1.8.1 MZI Switch

The Mach-Zehnder interferometer (MZI) based switch consists of a 3 dB splitter and a 3 dB combiner, connected by two interferometer arms. By changing the effective refractive index of one of the arms, the phase difference at the beginning of the combiner can be changed, such that the light switches from one output port to the other. This switch has the advantage that the phase shifting part and the mode coupling part are separated, such that both can be optimized separately. A small effective refractive index change in the interferometer is sufficient for the switching. The disadvantages are its length and the accurate refractive index change that is required for switching. When multimode interference couplers are employed as 3 dB splitter and combiner, a fabrication tolerant and polarization insensitive wave guiding structure is obtained.

Fig 1.5 Mach-Zehnder interferometer based switch

1.8.2 DC Switch

In a directional coupler switch two adjacent waveguides are designed such, that the light can be transferred from one waveguide to the other by coupling. The switching is obtained by properly adjusting the effective refractive index of one of the waveguides. For switching only a small refractive index change is needed. For a good transfer of the light, an accurate coupling length is required. Since this length is usually polarization and wavelength dependent and strongly influenced by fabrication deviations (etch depth, waveguide spacing), a good switch performance is hard to obtain.

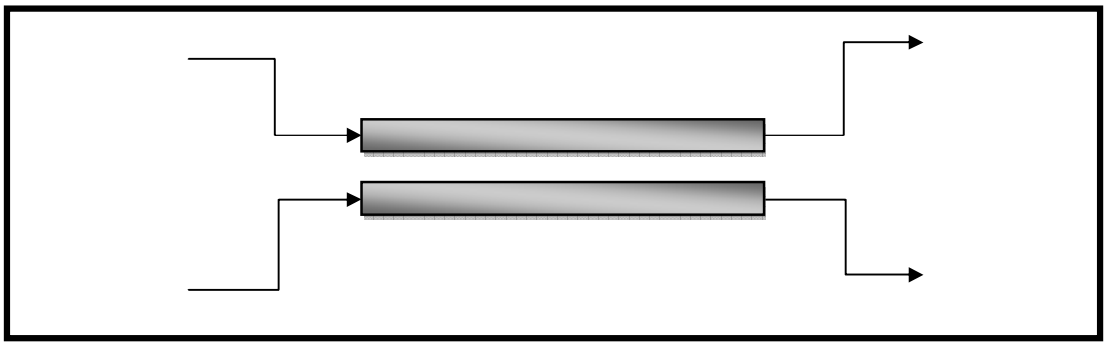

Fig 1.6 Directional Coupler Switch

1.8.3 SOA based MZI Switch

A semiconductor optical amplifier can both be used for amplification and attenuation of an optical signal, by turning the gain on and off. This property can be employed for a simple but effective way of switching by splitting an optical signal with a 3 dB splitter, after which this signal is attenuated in one arm and amplified in the other arm (Fig. 1.4). Since the splitter losses and additional losses (e.g. fiber-chip coupling loss) can be compensated by the SOA, this type of switch can have low loss or even gain and, in addition, excellent on-off ratios leading to low crosstalk levels [13]. The most important disadvantage of a SOA switch is its high additional noise level in the "on"state caused by spontaneous emission generated in the SOA [14].

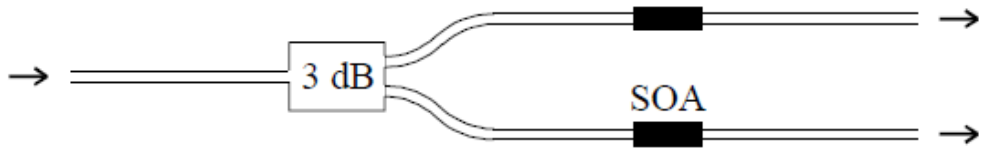

Fig 1.7 SOA based MZI Switch

1.9 Optsim Overview

Optsim is an advanced optical communication system simulation package designed for professional engineering and cutting-edge research of WDM, DWDM, TDM, CATV, optical LAN, parallel optical bus, and other emerging optical systems in telecom, data com, and other applications. It can be used to design optical communication systems and simulate them to determine their performance considering various component parameters. Optsim is designed to combine the greatest accuracy and modeling power with ease of use

on both Windows and UNIX platforms. Optsim represents an optical communication system as an interconnected set of blocks, with each block representing a component or subsystem in the communication system. As physical signals are passed between components in a real world communication system, “signal” data is passed between component models in the Optsim simulation.

1.10 Short Description of OptSim GUI Elements

(a) Title Bar

The title bar at the top of the OptSim window displays the name of the project currently opened. All projects must have filenames, therefore OptSim always asks you for a project to open or a name and location to save a new project when it is created.

(b) Menu Bar

Directly below the title bar, the menu bar groups most OptSim commands into Windows-style pull-down menus. Clicking on a pull-down menu will display a list of related commands.

(c) Tool Bar

The tool bar directly below the menu bar groups a set of buttons that serve as shortcuts for the most frequently used commands in the menu bar for editing related functions. Placing the cursor over a tool bar button causes a light-background box (tool tip) to popup with the name of the command executed by the button.

(d) Explorer

The explorer module provides access to the models library, models palettes, favorite schematics, user library, compound components library, and more. It also allows user to view a list of recent models or to see a panned view of the schematic in the design area.

(e) Design Area

The design area (layout pane) is the area below the tool bars where you may create the graphical network representing your design (either a compound component or complete

OptSim project). The grid shown in the figure may optionally be turned off or on by the user.

(f) Run Tools Bar

The run tools bar is a set of shortcut buttons for simulation run-related commands. It is located directly above the design area. Placing the cursor over a tool bar button causes a light-background box (tool tip) to pop up with the name of the command executed by the button.

(g) Toolbox

The toolbox is another set of shortcut buttons to access tools that are used in schematic drawing. These are not accessible from the menu. The toolbox is located on the left side of the design area. Placing the cursor over a tool bar button causes a light background box (tool tip) to popup with the name of the command executed by the button.

(h) Status Bar

The status bar at the bottom of the OptSim window is used to provide explanations and context-sensitive information regarding the status of the simulation that is currently running or other general project related information.

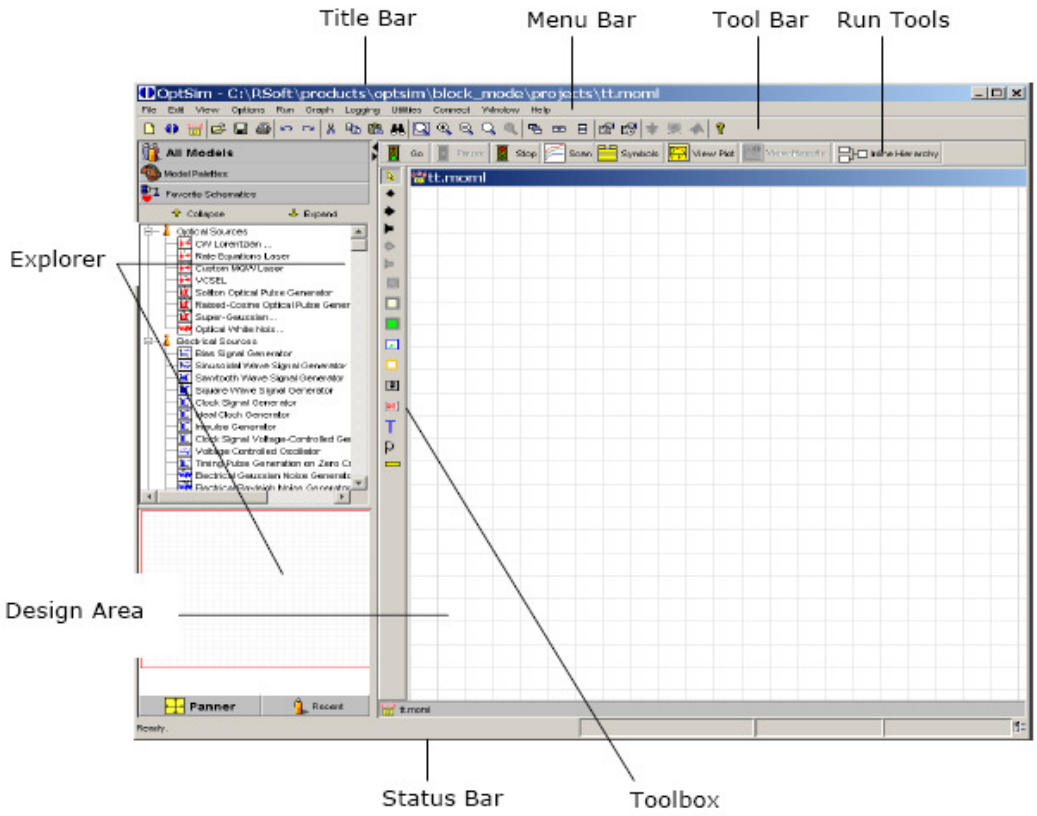

Fig.1.8 The OptSim graphical editor

Chapter 2

LITERATURE SURVEY

2.1 Literature Survey

Sang Hun Kim using the gain nonlinearity characteristics of semiconductor optical amplifier, an all-optical binary half adder at 10 Gb/s is demonstrated. The half adder operates in a single mechanism, which is cross gain modulation. The half adder utilizes two logic functions of SUM and CARRY, which can be demonstrated by using XOR and AND gates, respectively. The extinction ratios of both XOR and AND gates are about 6.1 dB. By achieving this experiment, here also explored the possibilities for the enhanced complex logic operation and higher chances for multiple logic integration.

A binary half adder [1] is a well known function in electronic gates and is a basis for enhanced complex processing circuits such as a full adder, a binary decoder, and a binary counter. As electronic circuits are anticipated to confront the speed limitation, efforts on the realization of all-optical logic systems are eventually increasing. Therefore, all-optical binary logic gates are expected to become a key technique in future communication networks. All optical binary half adders have been reported by using many optical designs such as terahertz optical asymmetric demultiplexers (TOAD) [2] and ultra-fast nonlinear interferometer [3]. All-optical logic device can be classified into several types such as the nonlinearity based on fibers [4-8], wavelength conversion based on a semiconductor optical amplifier, and so on. Comparing to techniques based on a fiber, wavelength conversion techniques based semiconductor optical amplifiers (SOA) [9-13] are attractive because of their high-gain, high saturation output power, wide-gain bandwidth, compactness, and integratibility with other photonic devices. The cross gain modulation (XGM) [14-18], one of several wavelength conversion techniques based on SOAs, is simple to implement and has shown impressive operation for a high bit rate. Moreover, the XGM shows a high conversion efficiency as well as insensitivity to the polarization of input signals. Our first binary half adder has been demonstrated previously [1]. However, past work utilizes two different mechanisms that are the XGM and cross-phase modulation (XPM) for XOR and AND operations, respectively. It is needless to mention that the system operating in a single mechanism has the definite advantages of high

compactness and integration possibility over multiple mechanisms. In this thesis experimentally demonstrate an all-optical half adder consisted of four SOAs using a single mechanism, which is the XGM.

Jitendra Nath Roy described Semiconductor optical amplifier (SOA)-based Mach–Zehnder interferometer (MZI) has already taken a significant role in the field of ultra- fast all-optical signal processing [18]. Optical tree architecture (OTA) provides important contributions in optical interconnecting networks. In this communication, tried to exploit the advantages of both OTA and SOA-based MZI switches. The proposed SOA-MZI-based tree architecture, a new and alternative scheme, for integrated all-optical logic and arithmetic operations. This architecture can enable one to perform all-optical processing of signals, including two input logic operations, half-adder, full-adder, full sub-tractor, one-bit data comparator, etc.

In this proposed scheme the significant advantage is that the operation of addition and subtraction is all-optical in nature. Beside this, logical operations can also be performed which are all-optical in nature. The same architecture can be used for different purposes. This scheme can easily and successfully be extended and implemented for any higher number of input digits by proper incorporation of MZI-based optical switches, vertical and horizontal extension of the tree and by suitable branch selection. Again, the whole operation is parallel in nature, i.e. the results of different operations between the data are obtained at a time. Here we can exploit the multiple instruction multiple data (MIMD) type operation nicely. Arithmetic operations can be conducted here between any two large-shaped data. The proposed one-bit digital data comparison scheme also successfully exploits nonlinear material-based tree structures for its operation. It is important to note that the above discussions are based on a simple model. In order to experimentally achieve results from the proposed scheme, some design issues have to be considered. For example, walk-of problem due to dispersion, polarization properties of fiber, predetermined values of the intensities/wavelength of laser light for control and incoming signals, introduction of filter, intensity losses due to beam splitters/fiber couplers, etc. Practical implementation of the suggested scheme will be reported in future work. CW beam of wavelength 1535 nm and pulsed signal of wavelength 1500 nm can be used as incoming and control signals, respectively. Intensity losses due to beam splitters/couplers in the interconnecting stage may not create much trouble in producing the desired optical bits at the output as the whole system is a digital one and the output depends.

Min Zhang et. al. demonstrates the current status and technologies of all-optical XOR gates. Various schemes with semiconductor optical amplifiers, particularly those associated with Interferometric structures, are discussed and compared. Finally, the applications of all-optical XOR gates to emerging networks are explored, and the future direction is outlined [19].

AO-XOR operation usually needs a nonlinear element to perform as a switching gate. A promising candidate among such nonlinear elements is the semiconductor optical amplifier (SOA) thanks to its practical advantages of high nonlinearity, low power consumption, short latency, high stability, and strong compactness. Furthermore, it can operate over the whole 1.3–1.6 μm wavelength window. Therefore, most of the reported XOR gates have used SOAs as nonlinear elements. These gates can be classified into two categories. In the first category, the gates depend on nonlinear effects in SOA itself, such as cross-polarization modulation (CPM), cross-phase modulation (XPM), cross-gain modulation (XGM), and four-wave mixing (FWM) This article has reviewed the current status and technologies of all-optical XOR gates. Very fine work is now emerging in the literature, but tough problems are still in the way before optical logic gates are able to compete with their electronic counterparts. Fiber-based XOR gates have been proven to be faster and pattern-insensitive but bulky in size, while compact SOA based ones suffer from the speed limitation induced by slow SOA gain recovery time. Those based on photonic crystal or active SOA waveguides with differential input schemes deserve more research attention. Future scientific breakthroughs to counteract the fundamental limitations of optics will most likely be made in new material and new structures.

Haijiang Zhang et. al. represented Both wavelength bi-stability (WB) and multiple bi-stability (MB) were predicted theoretically by Adams' model in resonant optical amplifiers. Their experimental observation in 850nm Vertical-Cavity Semiconductor Optical Amplifiers (VCSOA). Clockwise hysteresis of WB is observed at constant input power while the input wavelength is swept across the gain window. MB is observed at a fixed operation wavelength biased on the long wavelength side of the two separated Polarization-Dependent Gain (PDG) windows of the VCSOA by sweeping the optical input. The polarization of the input is set to a fixed angle with respect to the two intrinsic principal axes of the VCSOA. Two MB levels were experimentally observed at 160μW and 320μW, respectively. These observations are in good agreement with theoretical prediction by Adams' model and may lead to multi-valued optical information

manipulation.

Ivan T. Lima, et. al. propose a technique that uses Monte Carlo simulations with importance sampling and a reduced Stokes model to compute the probability density function of the Q-factor and the outage probability for a channel in a long-haul wavelength-division multiplexed optical-fiber transmission system due to the combination of polarization mode dispersion, polarization dependent loss, and polarization dependent gain [20]. This technique allows us to compute outage probabilities as small as 10^{-6} at a fraction of the computational cost required by standard Monte Carlo simulations.

The importance of sampling to efficiently and accurately calculate outage probabilities on the order of due to the combination of the polarization effects of PMD, PDL, and PDG using a reduced Stokes model, provided that the PMD is small enough that it does not distort the pulses within a channel. By using importance sampling, the time required can be reduce to compute small outage probabilities by three orders of magnitude when compared with standard Monte Carlo simulations. This result holds independent of the particular choice of receiver model. For currently improving the receiver model to include realistic filter shapes and to account for noise re-polarization during transmission[21].

J. P. R. Lacey et. al. describes Multichannel wavelength converters may be important components in the cross connects in future wavelength division multiplexed (WDM) transport networks. Here demonstrate a multichannel, polarization-insensitive, optically transparent wavelength converter, based on four-wave mixing in two semiconductor optical amplifiers in a polarization-diversity arrangement [21]. Bit-error-rate (BER) measurements with four input 2.5-Gb/s WDM channels, spaced by 2 nm, show penalties for wavelength conversion less than 2.6 dB at 10^{-9} BER. Changes in the state of polarization of the input signals cause the output power to change by less than 1.2 dB, and the corresponding power penalties change by less than 0.9 dB.

N. Pleros, et.al. describes the use of discrete but interconnected SOA–MZI switches for performing logical and highly functional processing tasks, demonstrating the multi-functional potential of the photonic switching elements is discussed[25]. An all-optical 3R burst-mode receiver consisting of four SOA–MZI switches and operating error-free with 40 Gb/s optical bursts, proving that interconnection of multiple switching units can lead to the realisation of key network node functionalities offering increased intelligence at the physical layer is presented. In order to allow for easier interconnectivity between the

SOA–MZI switches and to provide compactness and cost effectiveness to the developed subsystems, the integration of multiple switches into the same platform is proposed. To this end, the implementation of the first integrated quadruple SOA–MZI switch array is reported, increasing the integration density level and reducing packaging and pig tailing costs. Finally, possible applications of integrated multiple switch arrays are discussed, indicating their suitability for producing compact circuits performing common processing tasks in a multi wavelength environment, as well as their potential to lead to the development of an all-optical high speed packet switched node by implementing critical packet switching functionalities in a compact and efficient way.

After that they investigated the multi-functional potential of interconnected SOA–MZI switches and have also demonstrated the first integrated quadruple SOA– MZI switch array. The multi-functionality of interconnected gates has been confirmed by means of the demonstration of the first all-optical 3R burst-mode receiver circuit, which consists of four cascaded SOA–MZI switches and is shown to receive optical bursts error-free at 40 Gb/s directly in the optical domain. In order to facilitate interconnectivity and provide compactness and ease of use, the integration of multiple switching elements on the same chip has been proposed and the first quadruple SOA–MZI switch array has been presented, constituting the first step towards photonic integration density-level increment. Quadruple SOA–MZI switch arrays can in principle allow for four-channel processing procedures like wavelength conversion and 3R regeneration in a WDM system environment, by allocating one switching element for each discriminated wavelength. Finally, discussed possible applications of interconnected integrated multiple-switch arrays in packet/burst-switched architectures, and have shown that integration density-level increment opens the inroad towards the development and demonstration of an all-optical high-speed packet switched node.

Ghanshyam Singh, et. al. Presented a novel approach to the design of a 2x2 optoelectronic switch based on Mach-Zehnder interferometer. The designed model has a very high switching capability and is extremely reliable and has been devised keeping in view some inherent drawbacks like cost of higher driving voltage, high losses, polarization dependent losses and crosstalk's [26]. The various design parameters have been varied to improve the performance of the switch. A comprehensive study has been made on the effect of switching voltages on the switching properties with reference to the optical field propagation and refractive index propagation. However switch sizes larger than 2 x 2 can

be realized by appropriately cascading small switches. The main considerations in building large switches are number of small switches required, loss uniformity, number of cross over's and blocking characteristics.

In this review designed MZ interferometric 2x2 switches varying the simulation parameters to make a comparative study of the affect of these parameters on the switching capability. The measured crosstalk is lower than 27 dB at the branching angles of 0.2 and 0.3 for both the crossover and the straight through states. The switching voltage for the electrodes have been varied from 0.0 v to 6.75 volts which can be further lowered through the optimization of the waveguide structure For the realistic spatial switching systems which requires fabrication tolerance and reproducibility, the polymeric 2x 2 switch could be one candidate.

2.2 Thesis Objectives

In this thesis, the research is carried out keeping in the view of the following objectives.

1. To investigate the optical logical operation of Full adder using Mach-Zehnder Interferometer.
2. To investigate the bit error rate and quality factor for different states of polarisation at different channels.

2.3 Thesis outlines

After studying the basic introduction, literature survey and objectives of my thesis is define in chapter 2. In chapter three investigate the logical operation of full adder by using Mach-Zehnder Interferometer at very high bit rate. In Chapter 4 investigated the polarisation effect on wavelength division multiplexing for different states of polarisation. Finally discus the conclusion and future scope of this thesis in chapter 5.

Chapter 3

IMPLEMENTATION OF FULL ADDER USING MACH-ZEHNDER INTERFERO-METER

3.1 Introduction

As we know in recent days the research in optical computing increasing day by day and many scientists working upon them, but in electronics computing the logical operations plays a very important role because they require less power, as they are digital circuits and as compared to the analog circuits, they are very flexible. But they have certain disadvantage also that they work up to limited frequency, but if we used that logic using optical instruments then it gives better stability, better speed and switching. In digital optical computing, optical interconnecting systems are the primitives that constitute various optical algorithms and architectures. High speed all-optical logic gates are key elements in next-generation optical networks and computing systems to perform optical signal processing functions[1], such as all-optical label swapping, header recognition, parity checking, binary addition and data encryption. In the last few years, several approaches have been proposed to realize various logic gates using either high nonlinear fibers or semiconductor optical amplifiers (SOA) [2, 3]. The SOA-based devices have the potential of monolithically integration, which offer the advantages of compactness, increased reliability and cost reduction.

3.2 Tree architecture for all-optical full-adder

To implement OTA for triple-in-binary logic taken another four MZI-based optical switches s4, s5, s6 and s7 as shown in Fig.3.1. In this architecture the continuous wave laser source are falls on switch s1. For full adder three control signals is needed. Control signal A is given to the switch s1, control signal B is given to the switch s2 and s3 and control signal C is given to the switch s4, s5, s6, and s7. When the control signal is present then the light emerges upper channel and falls on the next channel and when the control signal is absent them light emerges from the lower channel followed by the next switch.

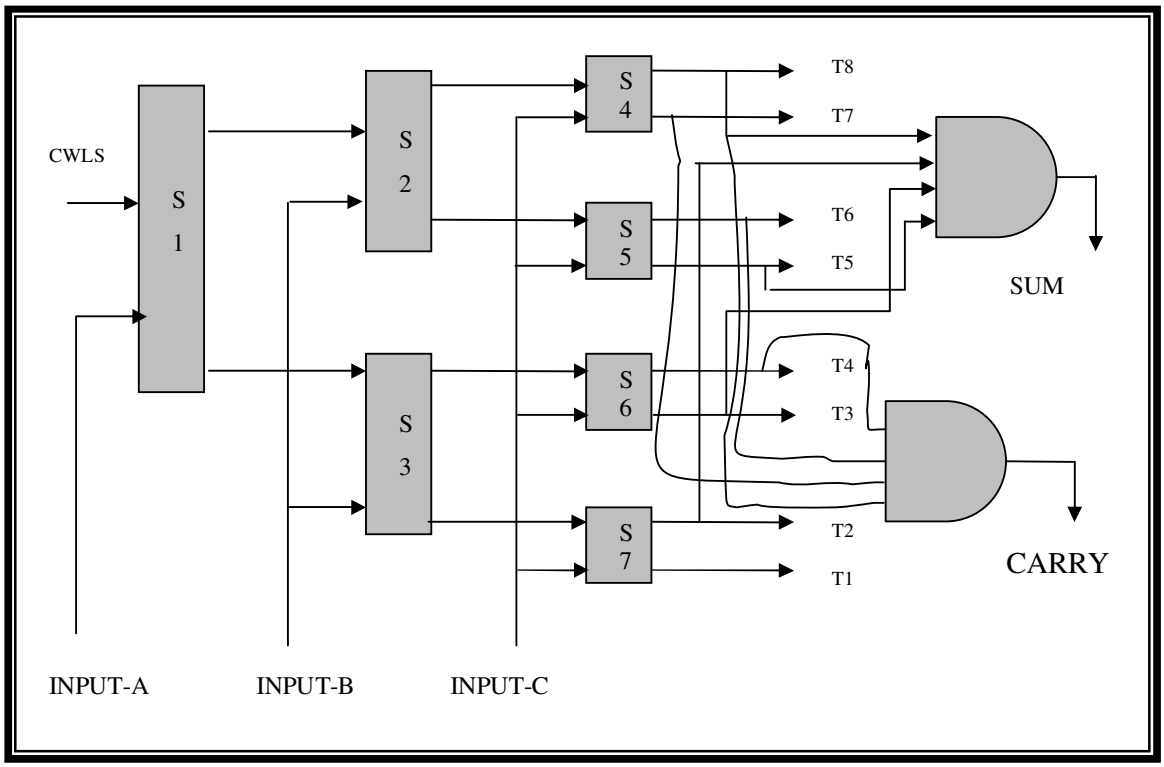

Fig 3.1 Optical circuit for integrated all-optical full adder

There are eight different input combinations for implementing triple input binary logic. Depending on the state of input variables (A, B, C) [these are also the light signals] the output is obtained from output terminal T-1 to output terminal T-8.

3.3 Theory of MZI

As the above full adder is implemented using SOA based MZI switch, so on the reference of that this chapter firstly describe the SOA based MZI switch. An MZI switch is a very powerful technique to realize ultra fast switching. In this switch a SOA is inserted in each arm of an MZI. The pulsed signal at the wavelength λ_1 is split at the first coupler such that more power passes through one arm. At the same time, the CW signal at the wavelength λ_2 is split equally by this coupler and propagates simultaneously in the two arms. In the absence of the λ_1 beam, the CW beam exits from the cross port (lower port in the figure). However, when both means are present simultaneously, all one bits are directed towards the bar port (upper port in the figure) because of the refractive-index change induced by λ_1 beam. The physical mechanism behind the behavior is cross-phase modulation (XPM).

Gain saturation induced by λ_1 beam reduces carrier density inside one SOA, which in turn increases the refractive index only in the arm through which the λ_1 passes. As a result, an additional π phase shift can be introduced on the CW beam because of the XPM, and the CW wave is directed towards the bar port during each one bit. Optical filters are placed in front of the output ports for blocking the original signal λ_1. The MZ scheme is preferable over cross gain saturation as it does not reverse the bit pattern and results in a higher on-off contrast simply because nothing exits from the bar port during 0 bit.

Now it is clear that in the absence of control signalλ_1, the incoming signal (CW signal) exits through the cross port (lower channel) of MZI. In this case no light is present in the bar port as shown in the below figure. But in the presence of the control signal, the incoming signal exits through the bar port of the MZI as shown in the figure. In this case no light is present in the cross port. In the absence of the incoming signal, the bar port and cross port receive no light as the filter blocks the control signal. [2, 4,]

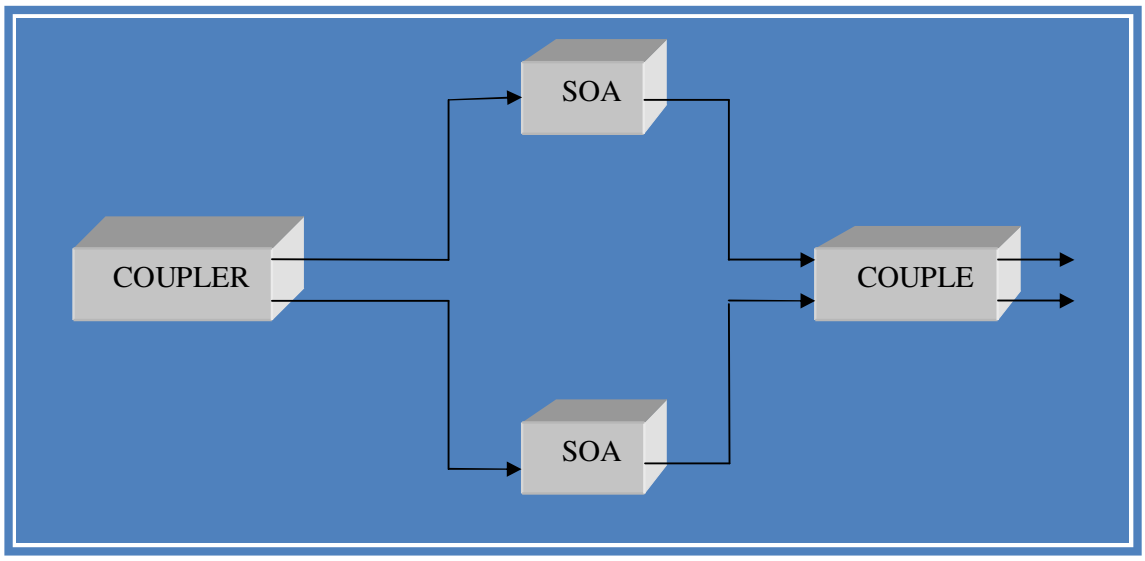

Fig 3.2 Block Diagram of Optical logic using MZ Interferometer Switch

3.4 Component Description

(a) Analog Sine Generator

This model creates an analog electrical signal representing a sine wave. It may be used to create a single sine wave, or a frequency comb of sine waves. In general, the output signal of this block can be described by the following equation

$$S_0(t) = V_{pp} \sum_{1}^{N} \sin\big((2\pi f_n t) + \varphi_n\big) + V_0$$

where so is the output signal value (whether it be in units of volts or amps depends on the setting of the signal Type parameter). Vpp is the peak to peak value of each sine wave in the frequency comb. N is the total number of frequencies summed together in the frequency comb. f_n is the frequency of each of the individual sine waves present in the frequency comb. t is the time. Φ_n is the phase offset for the nth element in the frequency comb. Vo is the offset value, which is added to the total signal after all sine waves in the frequency comb have been summed together.

Single Sine Wave Generator

When used as a single sine wave generator, the num Channels parameter is set to 1. The parameters in the Comb tab of the component parameters editing window are then unused. There are several ways in which this sine wave may be specified: as a Periodic sine wave, in which the signal start and end meet to produce a continuous periodic sine wave; or as an Aperiodic sine wave, in which the signal start and end do not necessarily meet to produce a continuous periodic sine wave. The primary difference between these approaches is how the time step (or alternatively, the sampling rate) and the number of data samples representing the signal are determined. The Periodic sine wave must be specified by setting the number of samples per period and number of periods. These settings along with the frequency determine the time step and the number of data samples. The Aperiodic sine wave must be specified by setting the time step, and number of data samples to represent the output signal. The number of periods which appear in the signal are then determined by the specified frequency, and the number of periods may be a fractional amount. The Periodic approach is most convenient except in cases where the signal will interact with other signals in the simulation which may have different frequencies and number of periods, resulting in different time steps and number of data samples. In these cases, the Aperiodic approach is most convenient because it allows the time step and number of data samples to be specified explicitly to match the other signals. When the Periodic approach is used, the user may easily view eye diagrams as the sine wave is mapped to a digital signal with a bit rate of twice the sine wave frequency and a number of bits equal to twice the number of periods specified.

(b)Direct Modulated Laser

This block models a semiconductor laser directly modulated with an electrical signal. It computes the electrical current injected into the laser's optical cavity and solves the laser rate equations for the optical output. The behaviour of the model can be partitioned into three blocks, as shown in Fig. 3.3. The driving source consists of the electrical signal input into the model. The parasitic consist of a bond inductance and shunting capacitance. Finally, the laser cavity is modelled via a simplified current-voltage (IV) relationship and the laser rate equations.

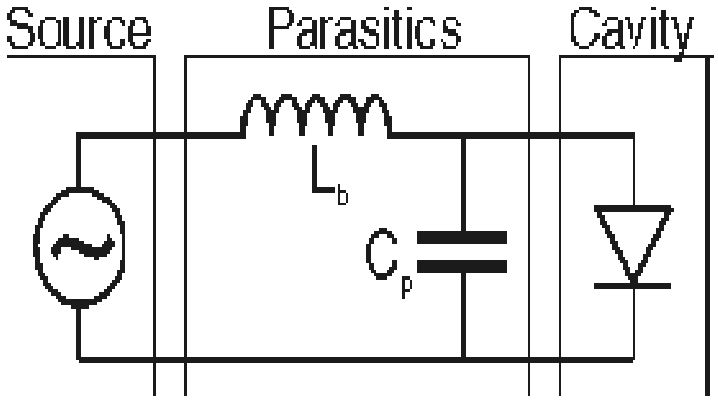

Figure 3.3: Main components of the Direct Modulated Laser model

Driving Source

The Direct Modulated Laser is driven by a combination of the electrical signal at its input and, when applicable, a dc bias current specified by Io (Io). Io can also be specified via a dc bias output power Po (Po). The user determines which will be used via the parameter Bias Value. The other parameter is then calculated automatically. The input electrical signal can be interpreted in a variety of ways, based on the settings of the model parameter Drive Scheme. This parameter can take on values of direct drive, bias tee.

(c) Optical Coupler (2x2)

This model represents an optical coupler. It takes an optical input signal on each port, and uses one of two ways to couple the optical signals together. If the **mode** is set to rameterized, it uses the following complex matrix to couple the signals, where A represents the complex optical field amplitude:

$$\begin{bmatrix} A_{01} \\ A_{02} \end{bmatrix} = \begin{bmatrix} \sqrt{1-\propto} & j\sqrt{\propto} \\ j\sqrt{\propto} & \sqrt{1-\propto} \end{bmatrix} \begin{bmatrix} A_{i1} \\ A_{i2} \end{bmatrix}$$

If the mode is set to Custom, the following complex matrix is used to couple the signals:

$$\begin{bmatrix} A_{01} \\ A_{02} \end{bmatrix} = \begin{bmatrix} C_{11} & C_{12} \\ C_{21} & C_{22} \end{bmatrix} \begin{bmatrix} A_{i1} \\ A_{i2} \end{bmatrix}$$

There is also a loss factor that may be applied to both input signals

(d)Semiconductor Optical Amplifier (SOA)

This module simulates a Semiconductor Optical Amplifier (SOA). The SOA is a highly nonlinear device. It can be used not only for signal amplification but also for other optical signal processing applications, such as wavelength converting, switching and optical time domain de-multiplexing [1]. The SOA is modelled as a travelling wave amplifier. It takes into consideration the time dependence of the gain caused by the saturation effect and the time-dependent phase change due to the gain-index coupling. Figure 3.4 shows a typical SOA geometry.

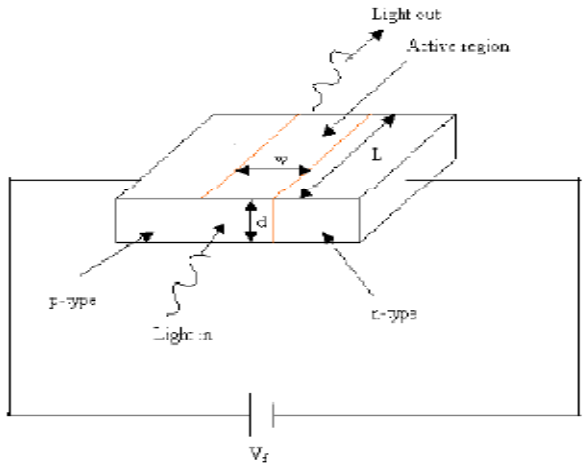

Figure 3.4: Typical SOA geometry

(e) Optical Filter

This model represents one of the following types of optical filters: Fabry Perot, Gaussian, Raised Cosine, Lorentzian, Trapezoidal, Ideal, Custom1, Custom2, and Custom3. Each

filter type except for the custom types may also be inverted. A wavelength signal whose filtered peak power does not exceed the user specified drop threshold will not be passed by the filter. The Trapezoidal filter type uses a Trapezoidal filter response to filter the optical signal amplitude. The user specifies the bandwidth in the wavelength domain (units of m) for the flat portion of the response as BW 0dB. The user also specifies the 3dB bandwidth in the wavelength domain. The Gaussian filter type uses a Gaussian filter response to filter the optical signal amplitude. The user specifies the 3dB bandwidth in the wavelength domain, and the order of the filter.

3.5 Simulation Results and Discussions

Case 1: When A =B=C=0

The light from CWLS Light from CWLS is incident on switch s1 [fig 3.5(a)]. As the control signal A is absent, the light emerges through the lower channel to fall on s_3. Due to the absence of control signal B here, the light follows the path of the lower channel and reaches switch s_7. Finally the light beam comes at output T-1 through the lower channel of $s_7$as the control signal C is absent. In this case only output terminal T-1 receives light, whereas the other seven output terminals do not receive any light. Hence T-1 is in one state and the others are in zero state, when A = B = C = 0.

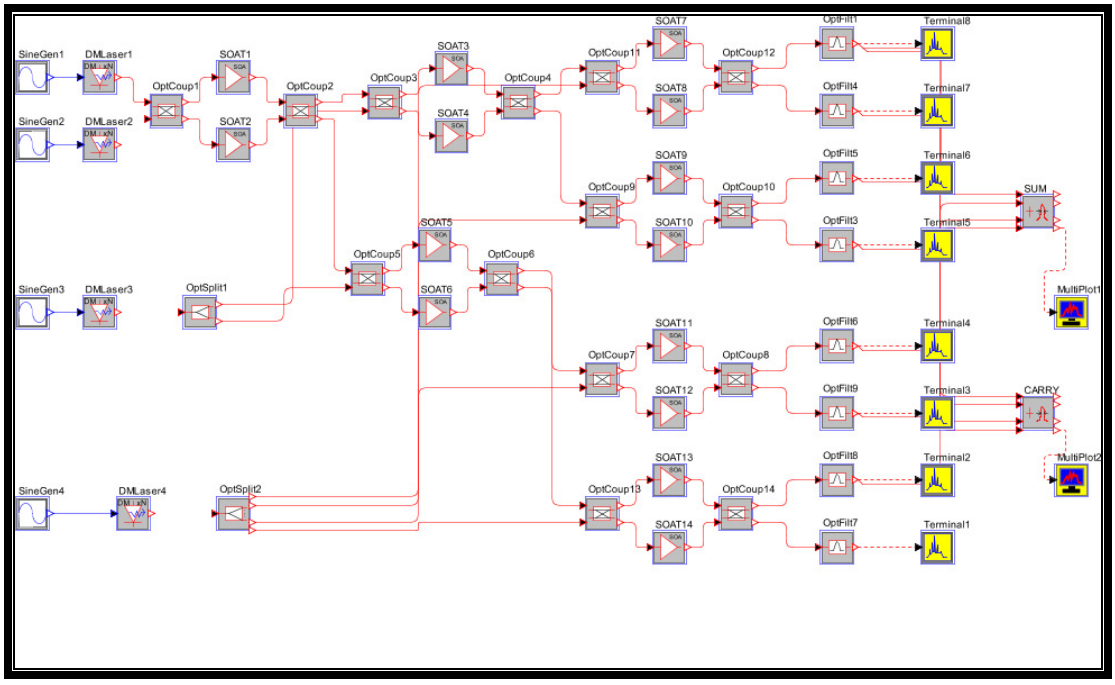

Fig 3.5(a) Simulation diagram of full adder for logic A=B=C=0

For getting sum combining the result of terminal -2, -3, -5, -8, and combining the result of terminal -4, -6, -7, -8 gives the result of carry. If the output power in wavelength spectrum is positive then that that result gives the high output, i.e. 1 and if the power in the wavelength spectrum is negative then that result is low output, i.e. 0. In this case output is high at terminal-1 but this output is connected to neither sum nor carry that so why the output of sum and carry gives very low power i.e. both gives the 0 output [fig 3.5(b)].

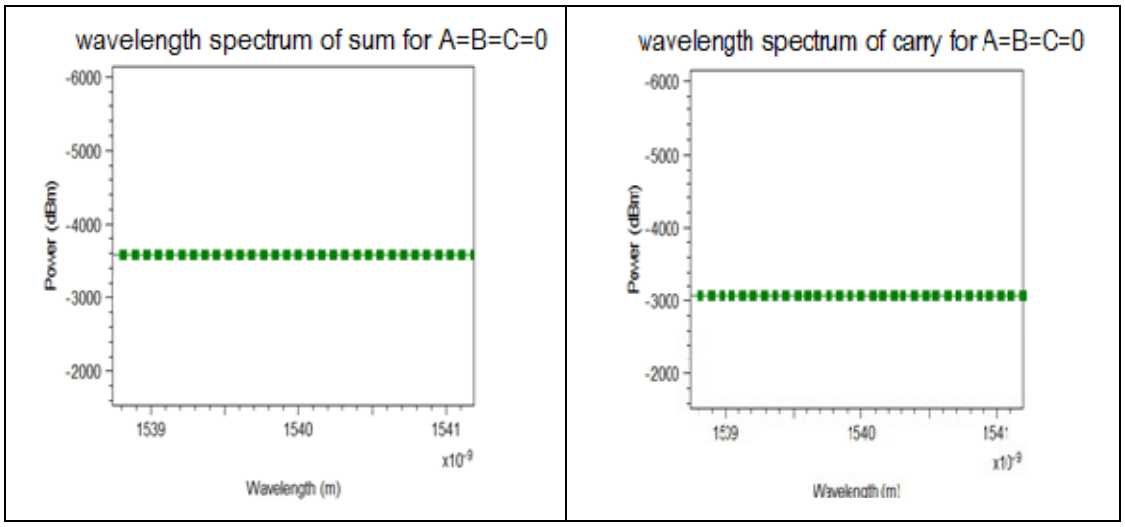

Fig 3.5(b) Wavelength spectrum of sum carry for logic A=B=C=0

Case 2: When A = 0, B = 0, C = 1

The light from CWLS Light from CWLS is incident on switch s1 [fig 3.6(a)]. As the control signal A is absent, the light emerges through the lower channel to fall on s_3. Due to the absence of control signal B here, the light follows the path of the lower channel and reaches switch s_7. Finally the light beam comes at output T-1 through the upper channel of s_6 as the control signal C is present. In this case only output terminal T-2 receives light, whereas the other seven output terminals do not receive any light. Hence T-2 is in one state and the others are in zero state, when A =0, B =0, C =1 . For getting sum combining the result of terminal -2, -3, -5, -8, and combining the result of terminal -4, -6, -7, -8 gives the result of carry. If the output power in wavelength spectrum is positive then that that result gives the high output, i.e. 1 and if the power in the wavelength spectrum is negative then that result is low output, i.e. 0. In this case the output of terminal-2 is high as a resulting spectrum for output of sum is high and for carry is low [fig 3.6(b)].

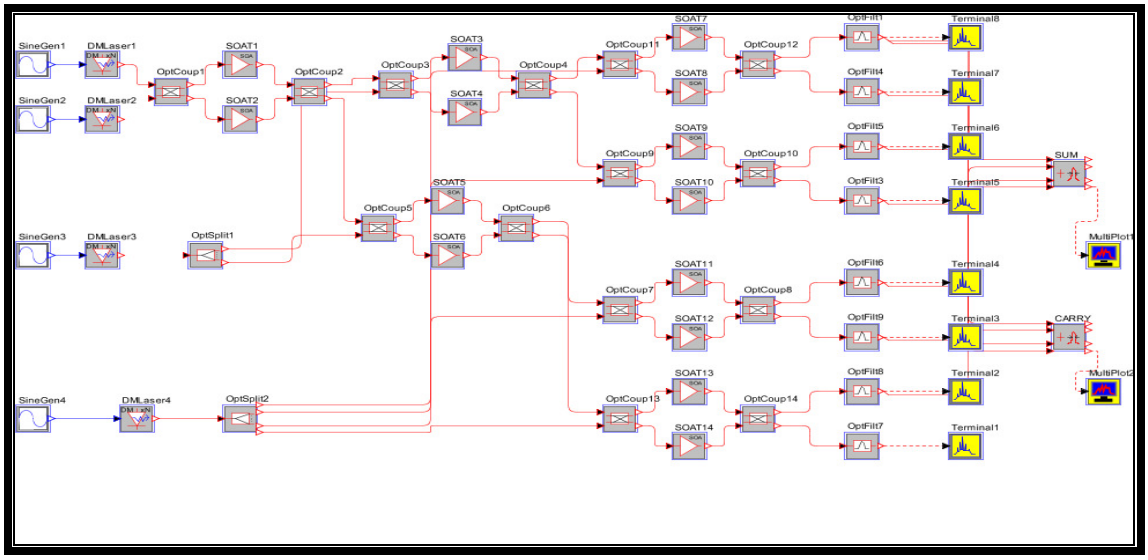

Fig. 3.6 (a)Simulation diagram of full adder for logic A=B=0,C=1

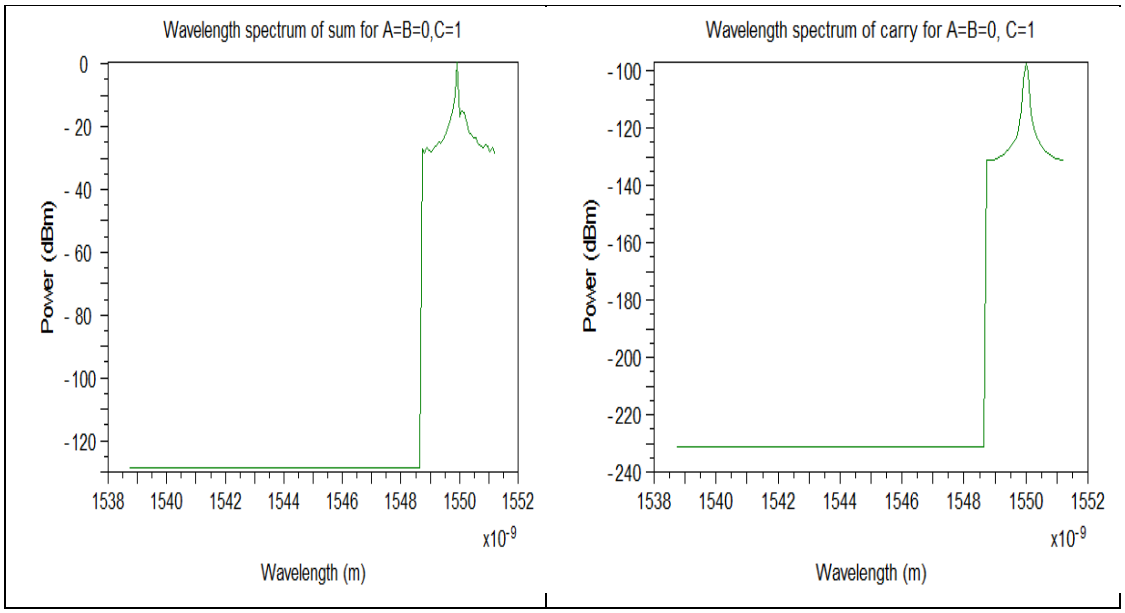

Fig3.6 (b)Wavelength spectrum of sum and carry for logic A=B=0,C=1

Case 3 A =0, B=1, C=0

The light from CWLS Light from CWLS is incident on switch s1 [fig.3.7 (a)]. As the control signal A is absent, the light emerges through the lower channel to fall on s_3. Due to the presence of control signal B here, the light follows the path of the upper channel and reaches switch s_6. Finally the light beam comes at output T-3 through the lower channel of s_6 as the control signal C is absent. In this case only output terminal T-3

receives light, whereas the other seven output terminals do not receive any light. Hence T-3 is in one state and the others are in zero state, when A =0, B =1, C = 0. In this case the output of terminal-3 is high as a resulting spectrum for output of sum is high and for carry is low [fig 3.7(b)].

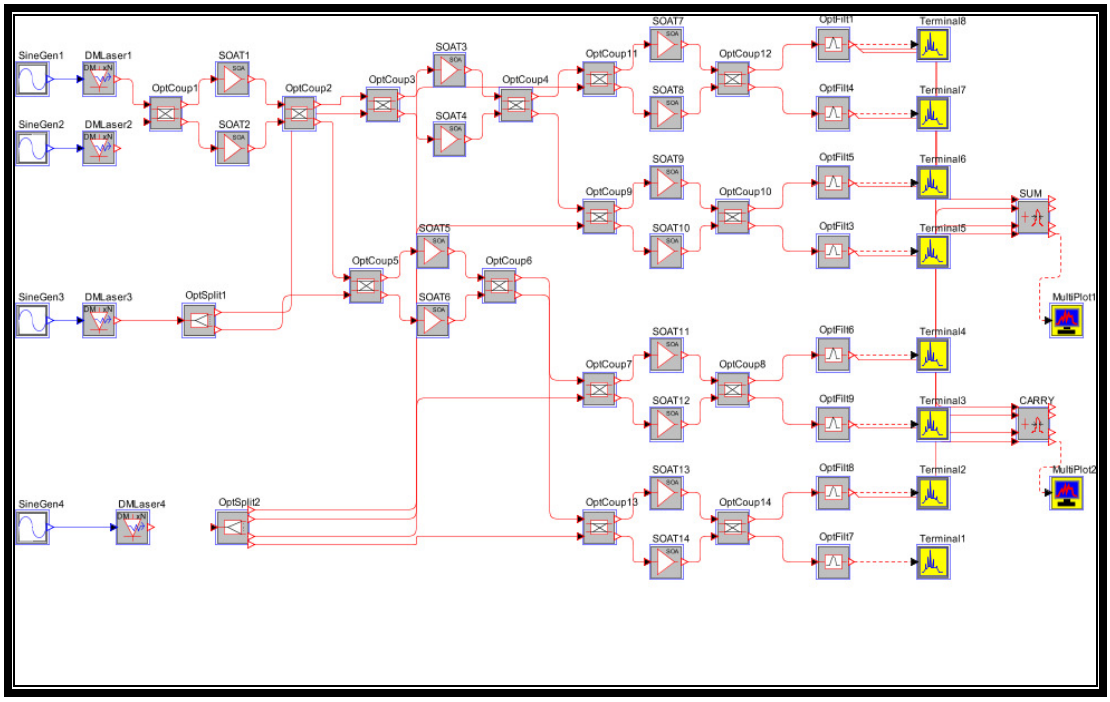

Fig. 3.7 (a)Simulation diagram of full adder for logic A=B=0,C=1

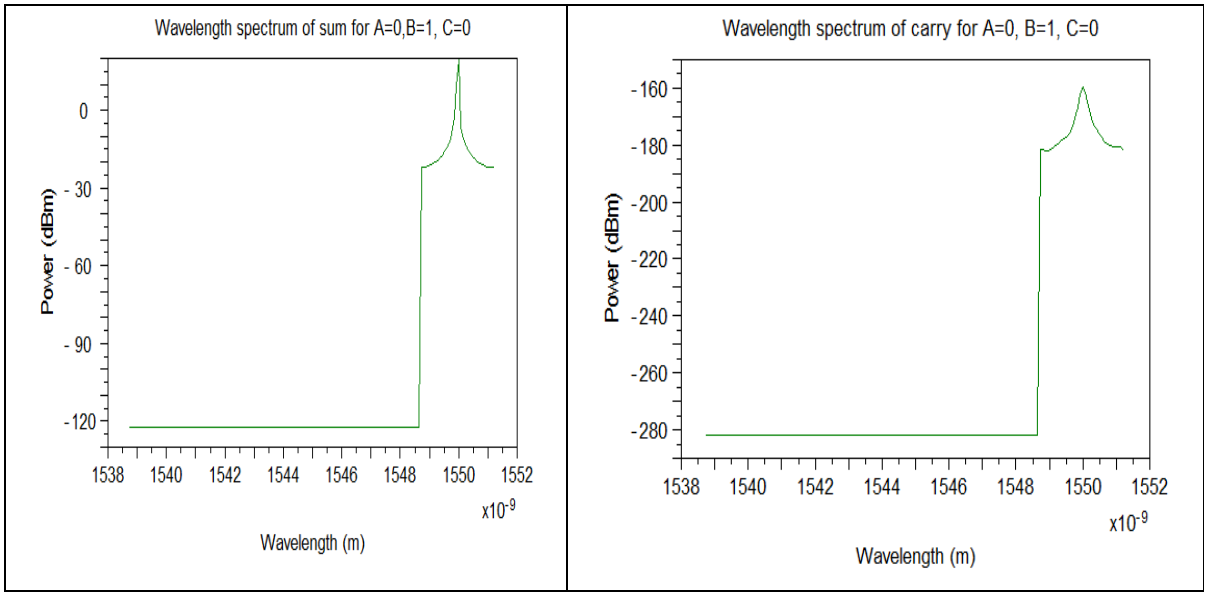

Fig3.7(b)Wavelength spectrum of sum and carry for logic A=B=0,C=1

Case 4 A=0, B=1, C=1

The light from CWLS Light from CWLS is incident on switch s1 [fig 3.8(a)]. As the control signal A is absent, the light emerges through the lower channel to fall on s_3. Due to the presence of control signal B here, the light follows the path of the upper channel and reaches switch s_6. Finally the light beam comes at output T-4 through the upper channel of s_6 as the control signal C is present. In this case only output terminal T-4 receives light, whereas the other seven output terminals do not receive any light. Hence T-4 is in one state and the others are in zero state, when A =0, B =1, C = 1. In this case the output of terminal-4 is high as a resulting spectrum for output of sum is low and for carry is high [fig 3.8(b)].

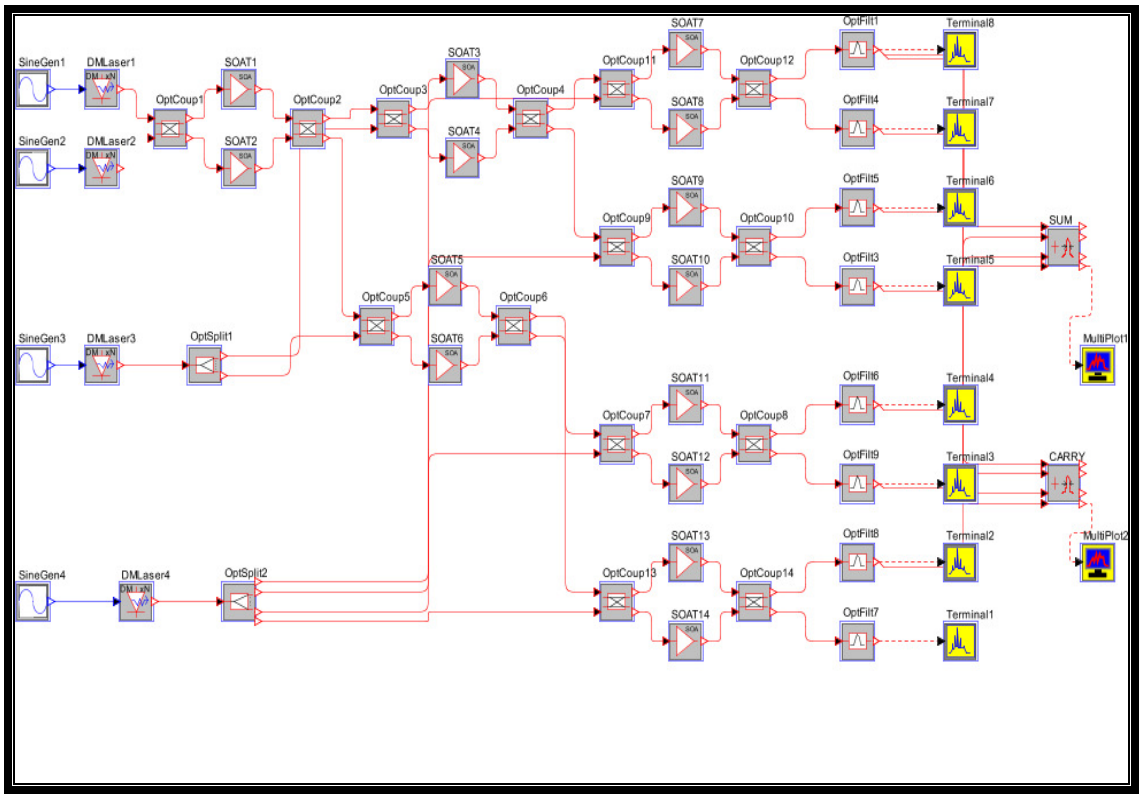

Fig. 3.8 (a)Simulation diagram of full adder for logic A=B=0,C=1

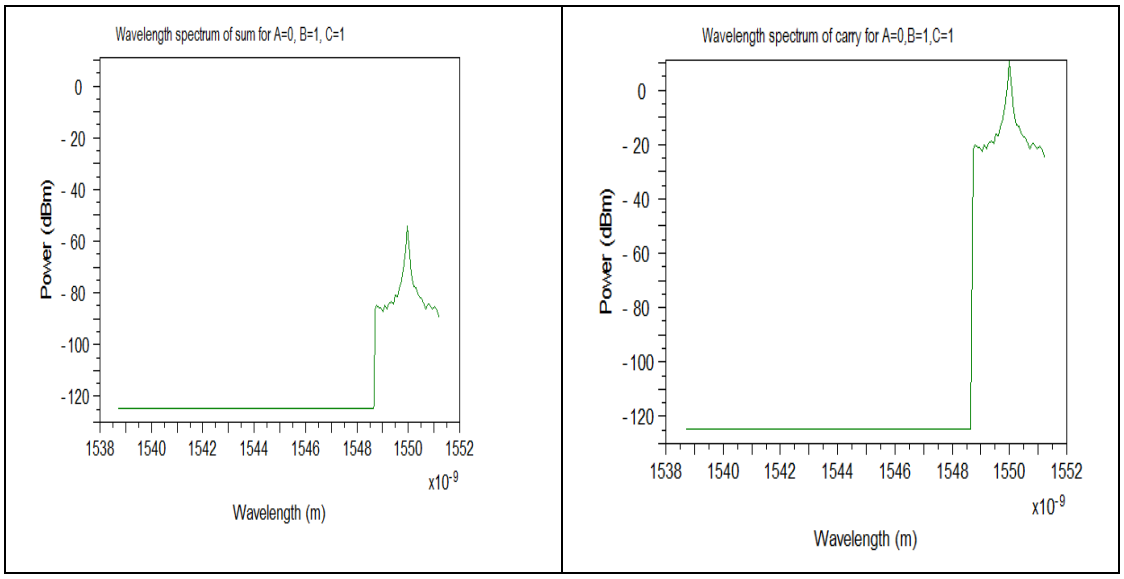

Fig3.8 (b)Wavelength spectrum of sum and carry for logic A=B=0,C=1

Case 5:A=1, B=0, C=0

The light from CWLS Light from CWLS is incident on switch s1 [fig 3.9(a)]. As the control signal A is present, the light emerges through the upper channel to fall on s_2. Due to the absent of control signal B here, the light follows the path of the lower channel and reaches switch s_5.

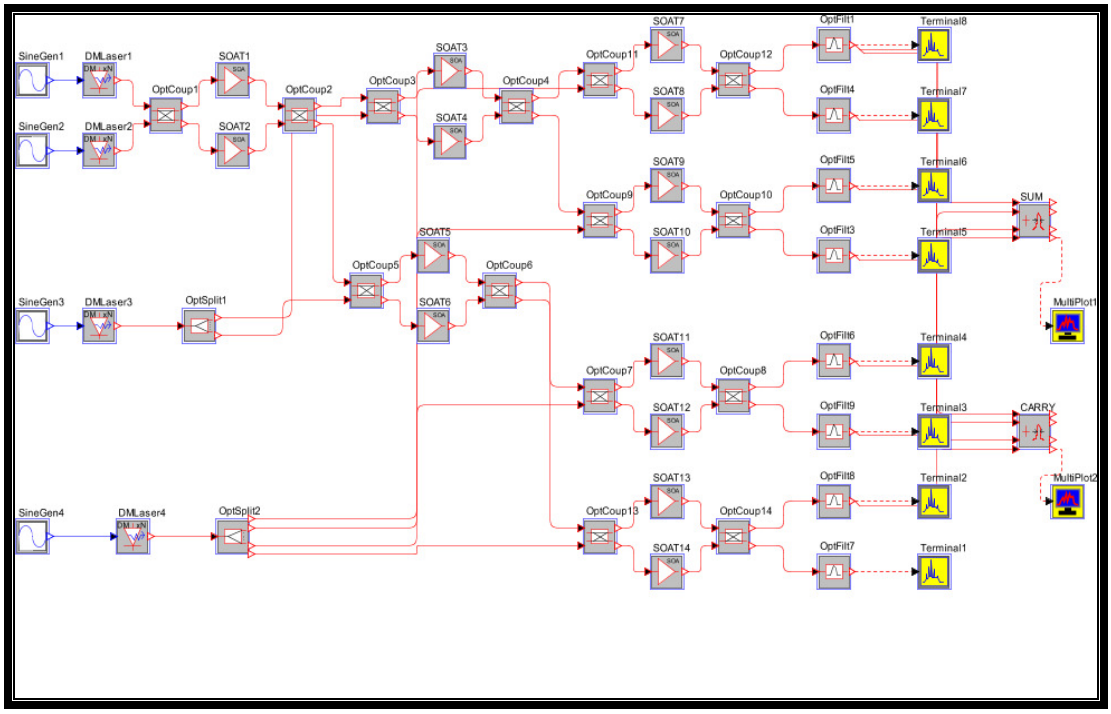

Fig. 3.9 (a)Simulation diagram of full adder for logic A=B=0,C=1

Finally the light beam comes at output T-5 through the lower channel of s_5 as the control signal C is absent. In this case only output terminal T-5 receives light, whereas the other seven output terminals do not receive any light. Hence T-5 is in one state and the others are in zero state, when A =1, B =0, C = 0. In this case the output of terminal-5 is high as a resulting spectrum for output of sum is high and for carry is low [fig 3.9(b)].

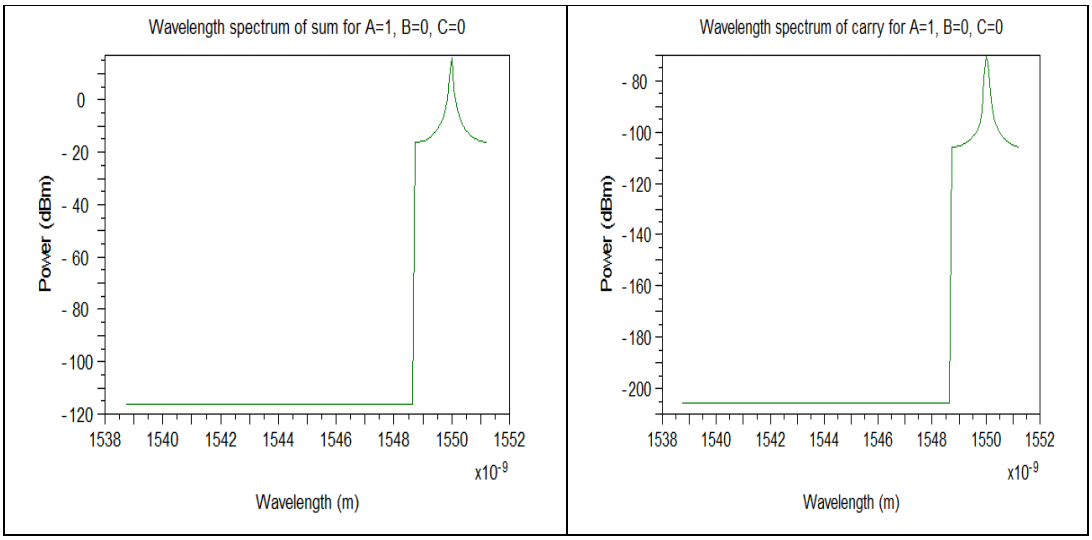

Fig3.9(b)Wavelength spectrum of sum and carry for logic A=B=0,C=1

Case 6: A=1,B=0,C=1

The light from CWLS Light from CWLS is incident on switch s1 [fig 3.10(a)]. As the

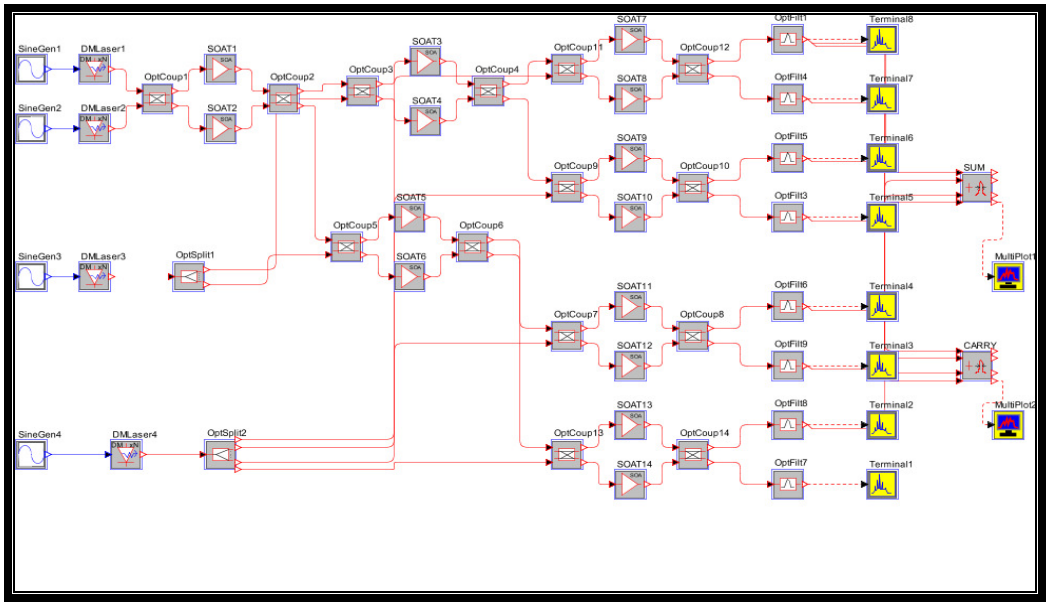

Fig. 3.10 (a)Simulation diagram of full adder for logic A=B=0,C=1

control signal A is absent, the light emerges through the upper channel to fall on s_2. Due to the absent of control signal B here, the light follows the path of the lower channel and reaches switch s_5. Finally the light beam comes at output T-6 through the upper channel of s_5 as the control signal C is present. In this case only output terminal T-6 receives light, whereas the other seven output terminals do not receive any light. Hence T-6 is in one state and the others are in zero state, when A =1, B =0, C = 1. In this case the output of terminal-6 is high as a resulting spectrum for output of sum is low and for carry is high [fig 3.10(b)].

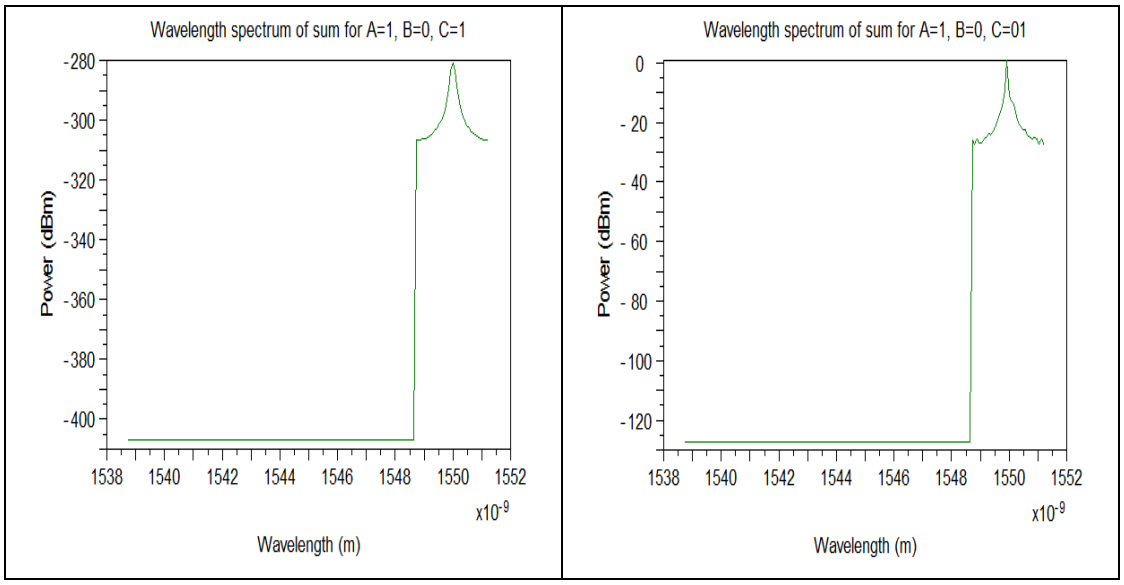

Fig3.10(b)Wavelength spectrum of sum and carry for logic A=B=0,C=1

Case 7:A=1, B=1, C=0

The light from CWLS Light from CWLS is incident on switch s1 [fig 3.11(a)]. As the control signal A is present, the light emerges through the upper channel to fall on s2. Due to the presence of control signal B here, the light follows the path of the upper channel and reaches switch s_4. Finally the light beam comes at output T-7 through the lower channel of s_4 as the control signal C is absent. In this case only output terminal T-4 receives light, whereas the other seven output terminals do not receive any light. Hence T-7 is in one state and the others are in zero state, when A =1, B =1, C = 0. In this case the output of terminal-7 is high as a resulting spectrum for output of sum is low and for carry is high [fig 3.11(b)].

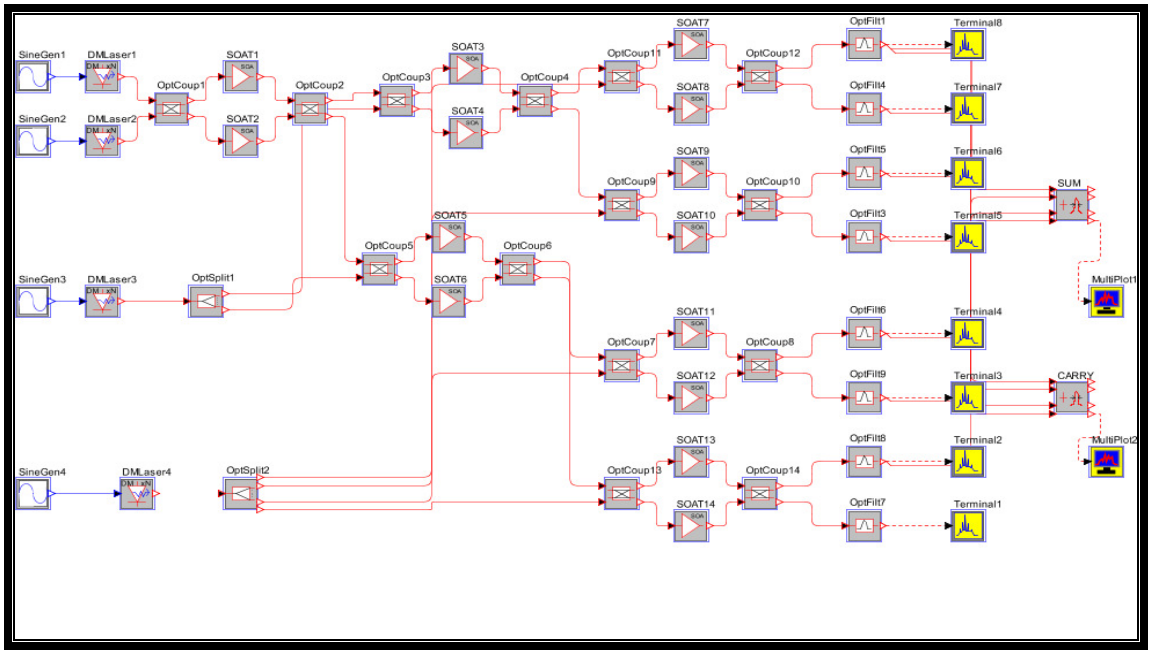

Fig. 3.11 (a)Simulation diagram of full adder for logic A=B=0,C=1

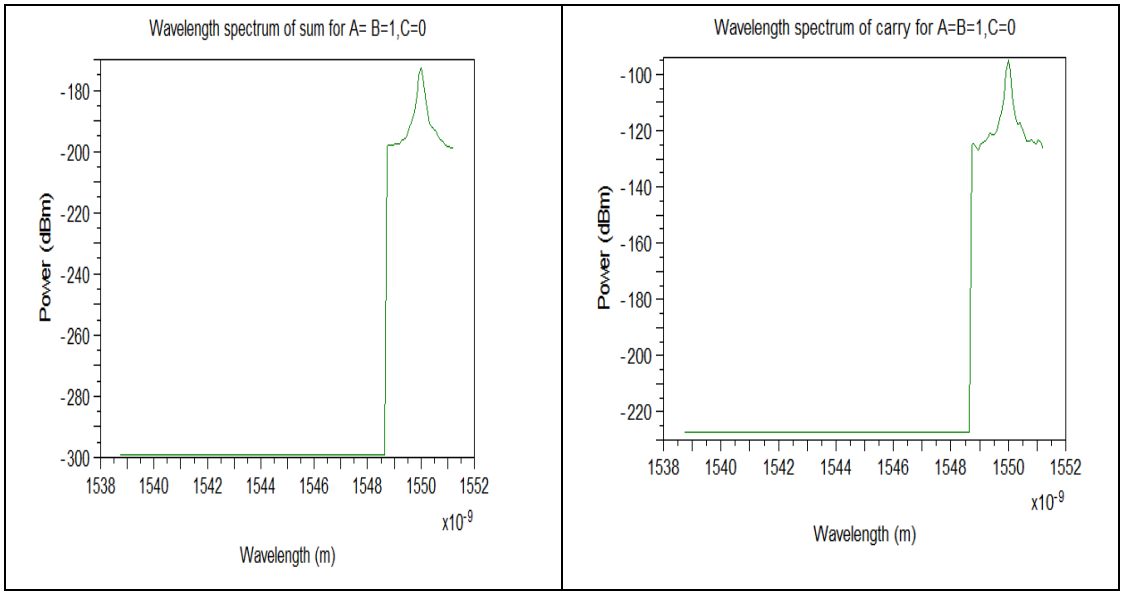

Fig3.11(b)Wavlengthe spectrum of sum and carry for logic A=B=0,C=1

Case 8: A=B=C=1

The light from CWLS Light from CWLS is incident on switch s1 [fig 3.12(a)]. As the control signal A is present, the light emerges through the upper channel to fall on s_2. Due to the presence of control signal B here, the light follows the path of the upper channel and reaches switch s_4. Finally the light beam comes at output T-8 through the upper channel of s_4 as the control signal C is present. In this case only output terminal T-8

receives light, whereas the other seven output terminals do not receive any light. Hence T-8 is in one state and the others are in zero state, when A =1, B =1, C = 1. In this case the output of terminal-8 is high as a resulting spectrum for output of sum and carry both are high output [fig 3.12(b)].

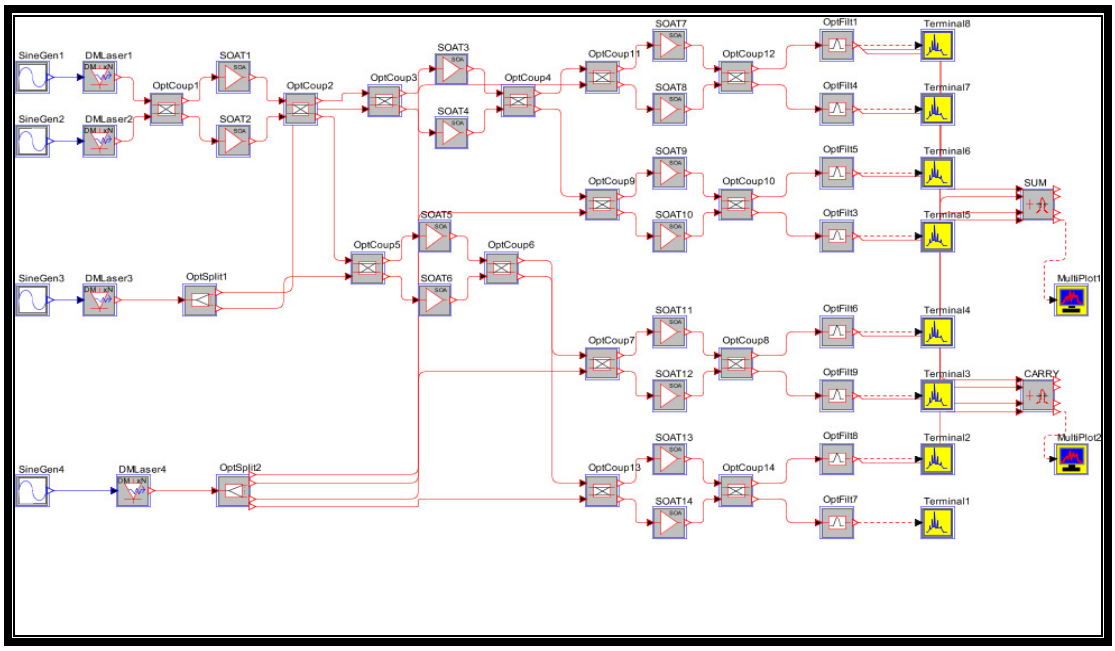

Fig. 3.12 (a)Simulation diagram of full adder for logic A=B=0,C=1

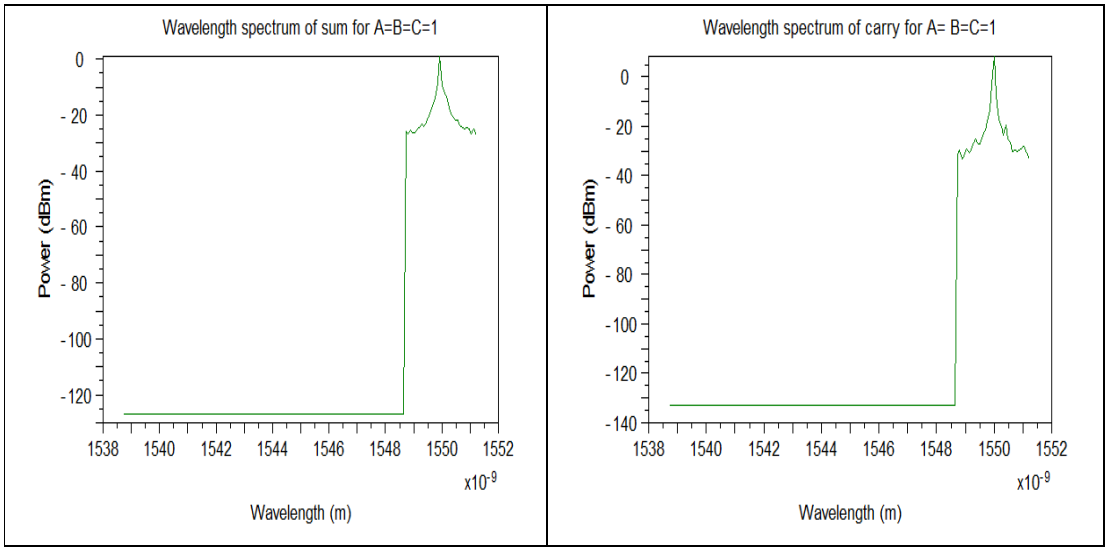

Fig3.12(b)Wavelength spectrum of sum and carry for logic A=B=0,C=1

Chapter 4

POLARIZATION EFFECT ON WDM

4.1 Introduction

Polarization is a property of waves that describes the orientation of their oscillations. This article primarily covers the polarization of electromagnetic waves such as light although other types of wave also exhibit polarization.

The introduction of wavelength converters into the cross-connects in WDM transport networks may allow improved blocking performance [23] and simpler network management. So-called optically transparent wavelength converters are modulation-format independent; and can perform multichannel wavelength conversion, in which a single wavelength converter simultaneously shifts the wavelengths of a comb of independently modulated wavelength-division multiplexing (WDM) channels. Large WDM cross connects based on multichannel wavelength converters may use fewer components and be more gracefully scalable than those based on single-channel wavelength converters [24]. An ideal multichannel wavelength converter is polarization insensitive; widely and arbitrarily tunable; and compact, because large arrays of wavelength converters may be required.

4.2 Un-polarized Light

Most sources of electromagnetic radiation contain a large number of atoms or molecules that emit light. The orientation of the electric fields produced by these emitters may not be statistical correlation, in which case the light is said to be "un-polarized". If there is partial correlation between the emitters, the light is "partially polarized". If the polarization is consistent across the spectrum of the source, partially polarized light can be described as a superposition of a completely un-polarized component, and a completely polarized one. One may then describe the light in terms of the degree of polarization, and the parameters of the polarization ellipse.

4.3 Polarization Effects in Everyday Life

Light reflected by shiny transparent materials is partly or fully polarized, except when the light is surface normal/perpendicular to the surface. It was through this effect that polarization was first discovered in 1808 by the mathematician Etienne Louis Malus. A polarizing filter, such as a pair of polarizing sunglasses, can be used to observe this effect by rotating the filter while looking through it at the reflection off of a distant horizontal surface. At certain rotation angles, the reflected light will be reduced or eliminated. Polarizing filters remove light polarized at 90° to the filter's polarization axis. If two polarizers are placed atop one another at 90° angles to one another, there is minimal light transmission.

Polarization by scattering is observed as light passes through the earth's atmosphere. The Rayleigh scattered light produces the brightness and colour in clear sky. This partial polarization of scattered light can be used to darken the sky in photographs, increasing the contrast. This effect is easiest to observe at sunset, on the horizon at a 90° angle from the setting sun. Another easily observed effect is the drastic reduction in brightness of images of the sky and clouds reflected from horizontal surfaces which is the main reason polarizing filters are often used in sunglasses.

4.4 Polarization on Channels

In wavelength division system there are number of channels launched into a single fiber span. Channel spacing is 50 GHz and they are generated in groups by odd and even channels by two PRBS generator. Initially all channels have the same polarization state. All even channels before being multiplexed with odd channels are passed through the Polarization Shifter, which rotates the polarization state by different angle. Fig.4.1 shows the block diagram of WDM system. After multiplexing the signal is launched into a fiber, and then is de-multiplexed and sent to 8 receivers. At the receiver end measure the BER and Q-factor for given polarization state difference between adjacent channels. There are two types of polarisation.

4.4.1 WDM Orthogonal Polarization

Here the polarization angle is scanned from 0 to 180 degrees with 10 degrees step and Q-factor is measured versus polarization angle.

4.4.2 WDM Random Polarization

Here the polarization angle is a randomly changing number with distribution statistics defined as uniform distribution within a range from –180 to +180 degrees.

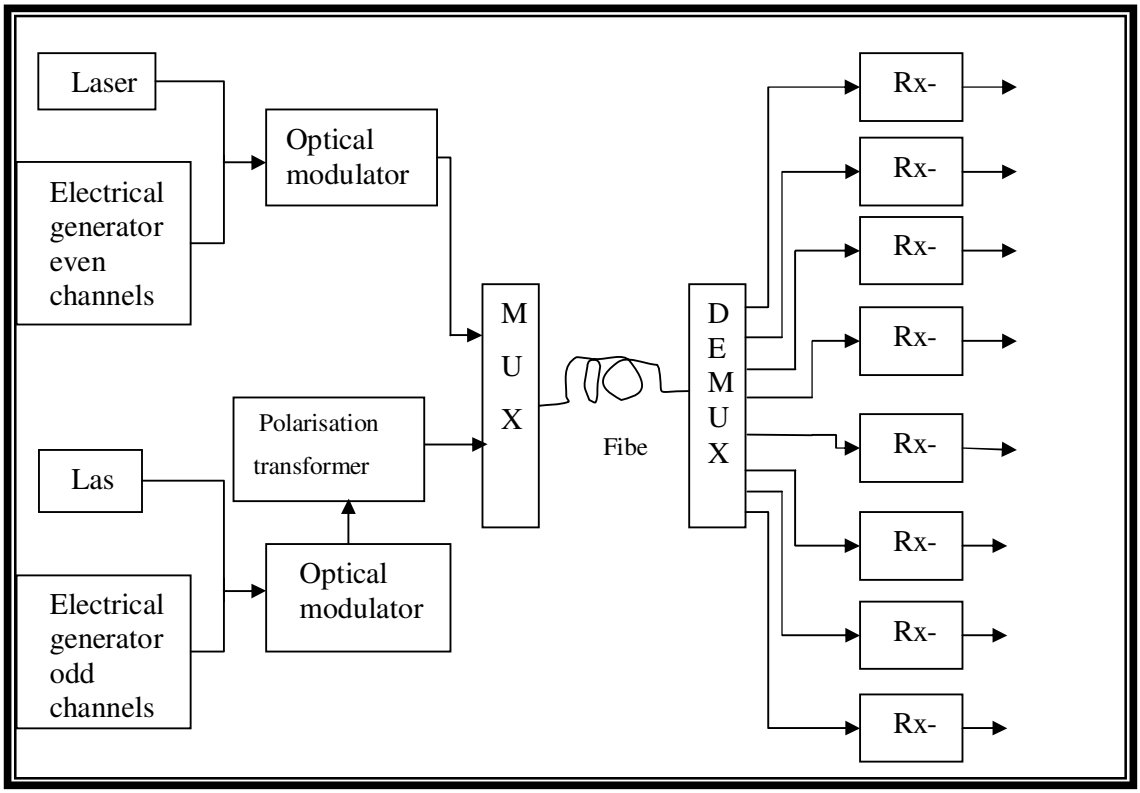

Fig 4.1 Block diagram of WDM system for different state of polarization

4.5 Component Description

(a) PRBS Pattern Generator

This model generates a binary sequence of several different types. A single model instance may be used to provide multiple pattern outputs, optionally offset from each other, to drive different channels of a WDM or parallel optical bus simulation. Or, each channel may have its own model instance configured to provide a different pattern than the other model instances. The different pattern types are described according to their name in the user parameter list:

(i) PRBS produces a maximal length pseudo-random binary sequence.

(ii) Alternating produces a series of bits alternating between 0 and 1.

(iii)Single produces a single 1 bit in the centre of a series of 0 bits.

(iv) One produces a series of 1 bits.

(v) Zero produces a series of 0 bits.

Custom: Produces a bit sequence as specified by the user in a data file. This file is to be placed in the directory in which the simulation will be performed, which is the directory in which the topology data file is located. This data file must be formatted as follows: Each line must contain 8 binary numbers separated by spaces. Each bit is represented as either '0' or '1'. There must be as many bits in the data file as are specified to be generated by the model.

Pre Bits and Post Bits

The bit sequence can be modified such that the first few bits (prebits) and the last few bits (postbits) are set to 0. This is useful in simulations because it increases the accuracy of the FFT when the begin and end of the sequence match. The default values should be sufficient for most applications.

(b) Electrical Signal Generator

This model converts an input binary signal into an output electrical signal. The output signal may be specified as either voltage or current. The user parameters are used to configure the electrical signal output. Four different electrical drive types are modelled, as described below.

On off: A square wave electrical signal is generated. No jitter is included in this square wave. For each bit period, the output signal data is set according to the value of the input bit and the voltage levels specified by the user: Vmax for a 1 bit and V_{min} for a 0 bit. After generation of this signal, it may optionally be passed through a ringing generation filter according to the user parameter setting for filter Type.

On off exponential: A square wave electrical signal is generated using the specified timing jitter. After the signal is generated, it is optionally passed through a ringing generation filter according to the user parameter setting for filter Type with specified rise time.

On Off Ramp: An electrical signal is generated using the specified rise time, fall time, and timing jitter. The signal rise and falls are ramped between the high and low levels.

After the signal is generated, it is optionally passed through a ringing generation filter according to the user parameter setting for filter Type.

Raised Cosine: An electrical signal is generated using a raised cosine shape to represent the binary signal. This signal includes the timing jitter, but does not include the user-specified rise and fall times because the signal shape is specified as a raised cosine. This signal type is not passed through the ringing generation filter. The duty cycle of the pulse may be varied from nearly 0% to 50% using the `alpha` parameter.

(c) CW Laser

This model produces the optical signal output of one or more CW lasers. It is most commonly used in conjunction with the external modulator model to encode a binary signal upon the CW source. In this model, the CW source is characterized completely by its power, wavelength, line width, relative intensity noise (RIN) and phase. These are controlled directly through the parameters peak Power, wavelength, line width, RIN and phase. The laser can also be assigned a random phase by setting random Phase=*YES*. There are two options for the temporal representation of the laser output selected by the parameter signal Type. For topologies in which a CW laser model provides direct input to a modulator model or the pumps of a Raman fiber amplifier, the Power Value signal representation is most convenient. In this representation, the optical signal holds a single complex value describing the field amplitude and phase. For topologies in which a CW laser model's output is used as input to other component models or is to be multiplexed with different optical signals from other types of sources, the Time Sequence signal representation should be used. This is the standard time-sampled representation of optical signals. For this representation, the time Step and no Samples parameters must be set appropriately to match the sampling rate and number of data samples of any other signals with which it will interact in the simulation. The nominal Bit Rate parameter should also be set to an appropriate data rate.

(d) Electroabsorption Modulator

This model represents an electroabsorption modulator. It allows the user to specify the extinction ratio of the output optical signal explicitly, and it scales the input modulating voltage signal as required to obtain the specified extinction ratio at the output. Nonlinear modulation response is also supported with either file-based data interpolation or a 7^{th} order polynomial in terms of the scaled input modulating voltage signal. The model also

allows the chirp factor to be specified as a data file or as a 7th order polynomial in terms of the input modulating voltage signal and supports specification of dc chirp with another data file or 7th order polynomial in terms of the input modulating voltage signal. In addition, the user may specify whether or not the output optical signal should be modulated as the inverse of the input electrical signal, and whether the alpha parameter should be considered positive or negative (to accommodate differing conventions in the literature). The model has two input ports and one output port. The first input port accepts an optical signal that is modulated to produce the output optical signal, and the second input port accepts an electrical signal that is used to modulate the input optical signal to produce the output optical signal. The input optical signal may be any type of optical signal, but it is recommended to use the CW laser or mode-locked laser sources to provide the input optical signal. The user must ensure that the total number of samples contained within the input electrical and optical signals is the same, as are the sampling rates. An exception to this is when using the CW laser model to produce the Power Value signal type.

(e) Compound Optical Receiver

This models an optical receiver and all its standard parts. The OptSim photo receiver model is composed of several individual building blocks: the photo detector, the preamplifier, and the post amplifier/filter complex

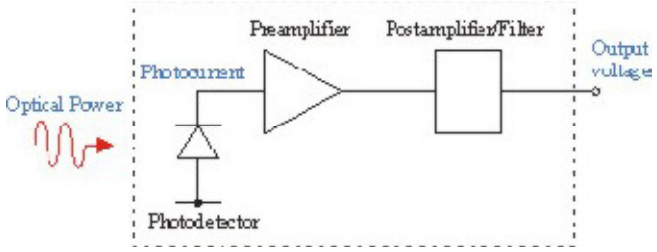

Figure 4.2: Basic components of an optical receiver

Each block is a separate entity complete with its own input parameters and options. The photo detector model converts an optical input signal to an electrical current. This photocurrent is then passed to the preamplifier model which converts it to a voltage. Finally, the post amplifier model contains a set of baseband filters that shape the output waveforms. The model also computes the photo receiver noise components. In fact the receiver model is implemented directly in terms of the three stand-alone models the PIN/APD Photo detector, Electrical Amplifier and Electrical Filter model described

elsewhere in this manual and all the parameters of each of those models are also parameters of the monolithic receiver model. In other words the two configurations shown in the topology in Figure 4.2 serve equivalent functions. There are two motivations for providing this additional receiver model. As a matter of convenience and topology compactness, some users may find it useful to represent the receiver configuration with a single block. However, this function could also have been achieved by creating a super-block containing the three individual models. Rather, the principal reason for providing a combined model is to allow a "Quasi-Analytic" (QA) treatment of the receiver noise. Both the photo detector and electrical amplifier model a number of noise sources – shot noise, dark current noise, signal spontaneous emission beta noise, thermal noise in the pre-amp transistor etc. In these two models, the noise is added directly as a stochastic contribution to the electrical signal – the so-called Monte-Carlo (MC) picture.

4.6. Simulation Setup for Polarization Effect on WDM

The topology setup Fig 4.3 consists of 8 channels launched into a single fiber span. Channel spacing is 50 GHz and they are generated in groups by odd and even channels by two PRBS generators, Electrical Signal Generators, and CW laser sources.

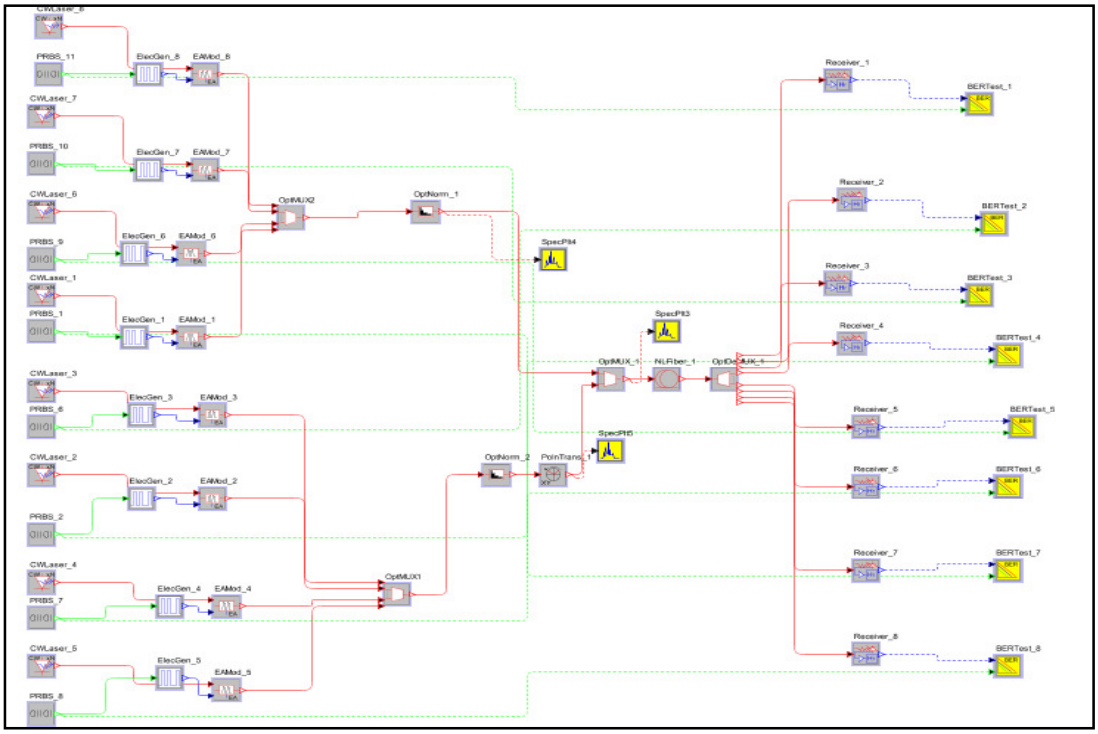

Fig 4.3 Simulation setup for polarization dependence studies

All even channels before being multiplexed with odd channels are passed through the Polarization Shifter, which rotates the polarization state by different angle. After multiplexing the signal is launched into a fiber, and then is de-multiplexed and sent to 8 receivers followed by BER Tester to measure channel performance (BER and Q-factor) for given polarization state difference between adjacent channels. Initially all channels have the same polarization state.

4.6. Results and Discussion

Here following points discuss the one odd channel and one even channel for different length of fiber at orthogonal polarisation.

4.6.1 Polarisation State for Fiber Length of 75 km

Here the polarization angle is scanned from 0 to 180 degrees with 10 degrees step and Q-factor is measured versus polarization angle. Figure 4.4 shows results for one odd (chanel3) and Figure 4.5 one even channel (chanel6). In both cases the Q-factor is minimal for polarization angles equal to 0 or 180 degrees, i.e. when all channels have parallel polarization states; and Q has maximum at 90 degrees, i.e. when adjacent channels polarization state is orthogonal to each other. Difference between max and min Q's is 0.607- 0.703 dB for these cases. The BER has minimum value at 90 degree, i.e. when adjacent channels polarization state is orthogonal to each other. Difference between max and min BER is 2.955 x 10^{-8} – 5.9043 x 10^{-8} for these cases.

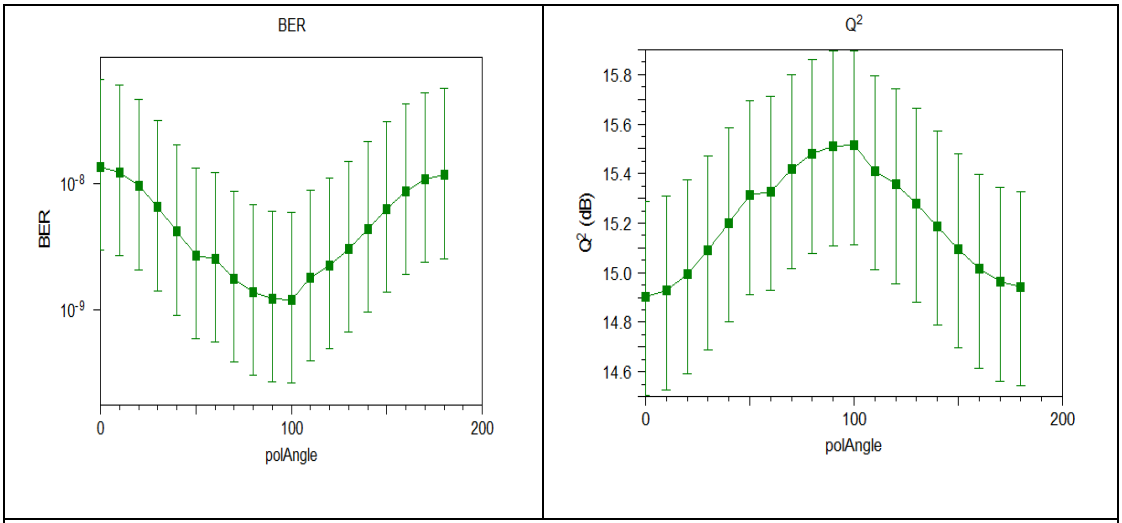

Fig.4.4 BER and Q-factor versus polarization angle for Odd channel (channel-3)

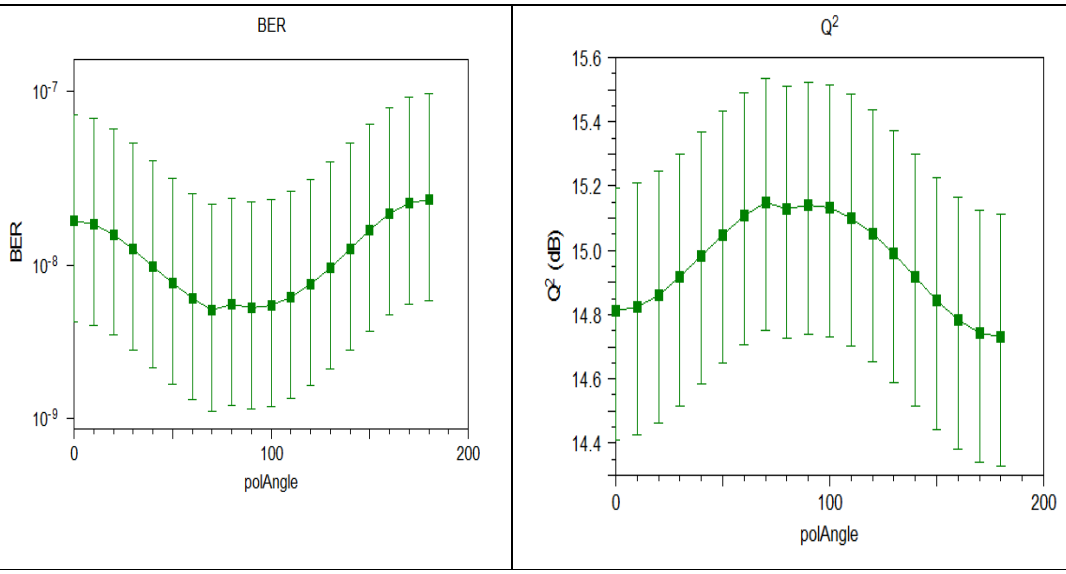

Fig.4.5 BER and Q-factor versus polarization angle for even channel (channel-6)

4.6.2 Polarisation State for Fiber Length of 80 km

Here the polarization angle is scanned from 0 to 180 degrees with 10 degrees step and Q-factor is measured versus polarization angle. Figure 4.6 shows results for one odd (channel-3) and Figure 4.7 one even channel (channel-6). In both cases the Q-factor is minimal for polarization angles equal to 0 or 180 degrees, i.e. when all channels have parallel polarization states; and Q has maximum at 90 degrees, i.e. when adjacent channels polarization state is orthogonal to each other. Difference between max and min Q's is 0.275 to 0.635dB for these cases.

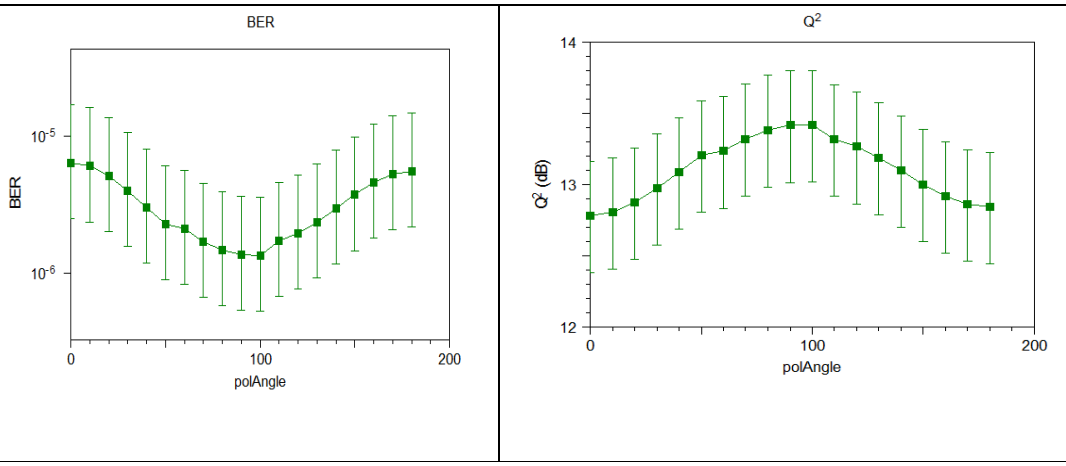

Fig.4.6 BER and Q-factor versus polarization angle for Odd channel (channel3)

The BER has minimum value at 90 degree, i.e. when adjacent channels polarization state is orthogonal to each other. Difference between max and min BER is 2.894 x 10^{-6} – 5.2406 x 10^{-6} for these cases.

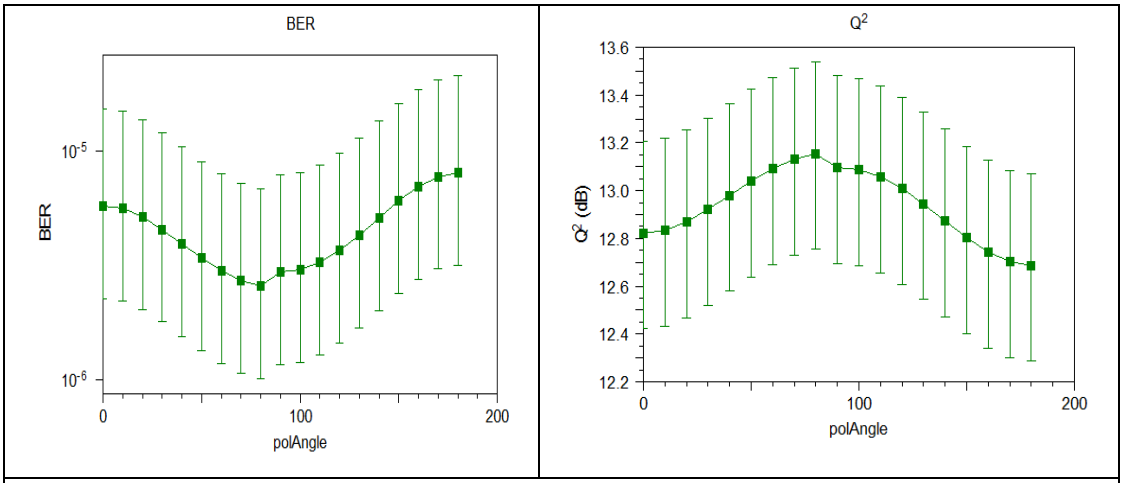

Fig.4.7 BER and Q-factor versus polarization angle for even channel (channel6)

4.6.3 Polarisation State for Fiber Length of 85 km

Here the polarization angle is scanned from 0 to 180 degrees with 10 degrees step and Q-factor is measured versus polarization angle. Figure 4.8 shows results for one odd (channel-3) and Figure 4.9 one even channel (channel-6). In both cases the Q-factor is minimal for polarization angles equal to 0 or 180 degrees, i.e. when all channels have parallel polarization states; and Q has maximum at 90 degrees, i.e. when adjacent channels polarization state is orthogonal to each other. Difference between max and min

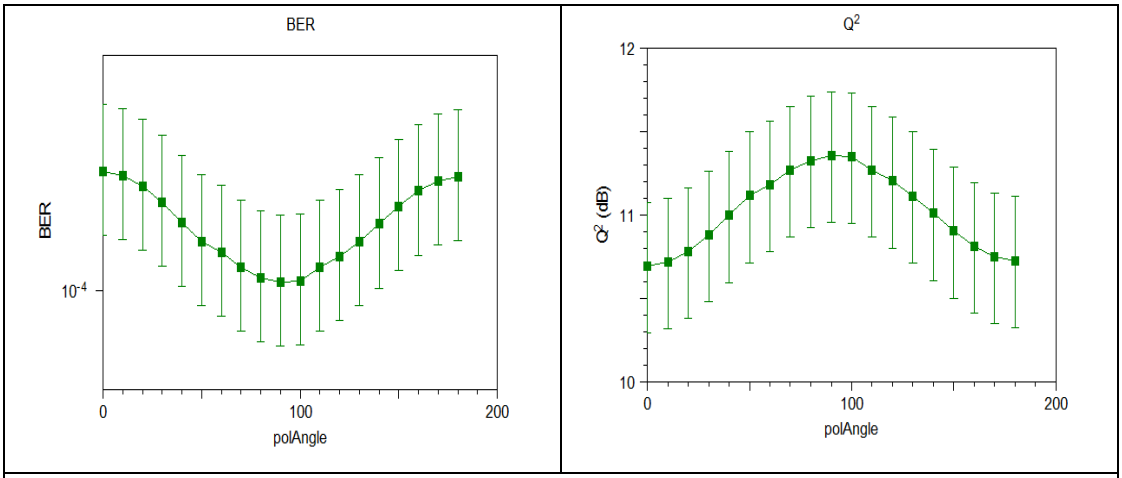

Fig.4.8 BER and Q-factor versus polarization angle for Odd channel (chanel-3)

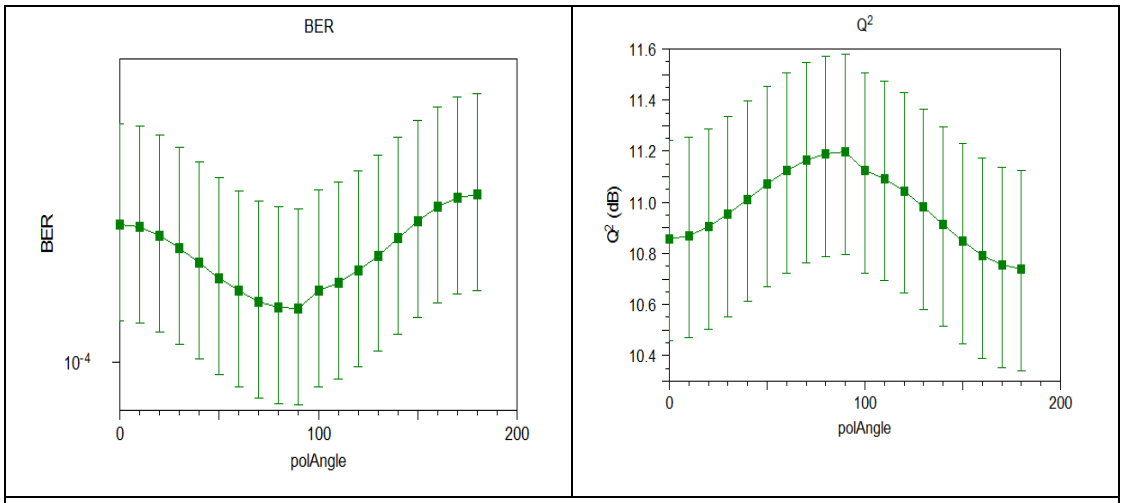

Fig.4.9BER and Q-factor versus polarization angle for even channel (channel-6)

Q's is 0.275 to 0.635dB for these cases. The BER has minimum value at 90 degree, i.e. when adjacent channels polarization state is orthogonal to each other. Difference between max and min BER is 2.894 x 10^{-6} – 5.2406 x 10^{-6} for these cases.

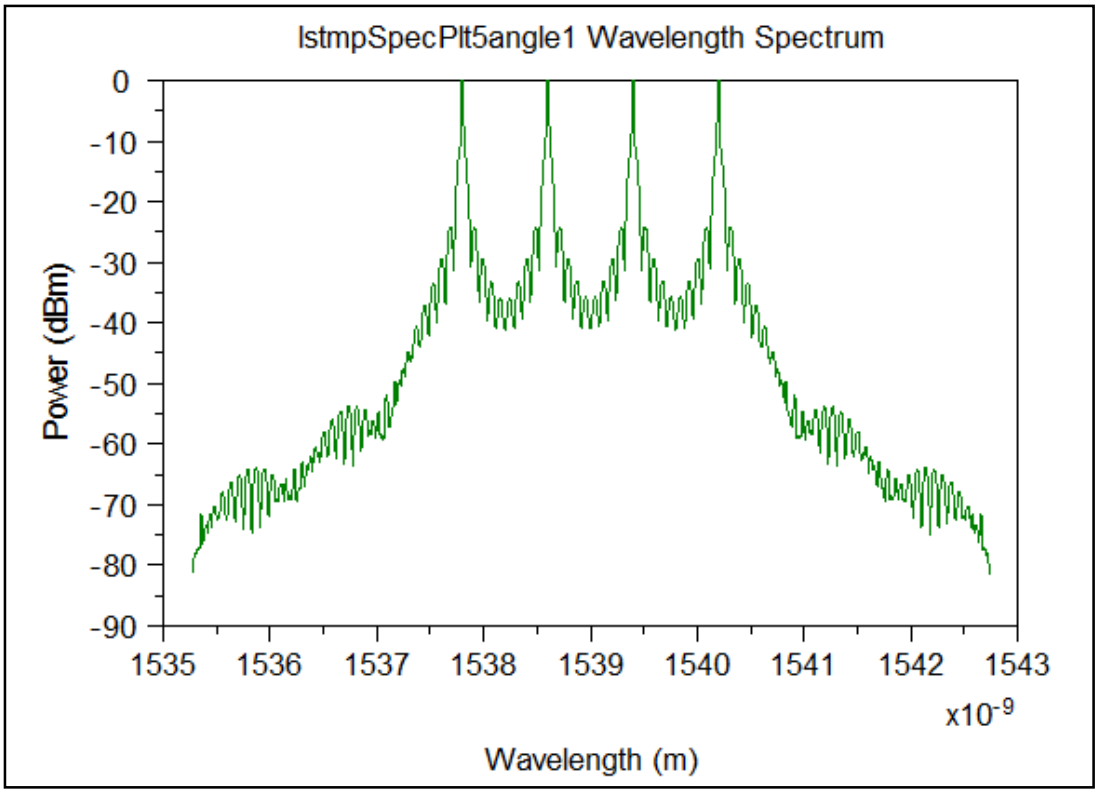

Fig 4.10 Wavelength spectrum after polarization transformer for odd channel

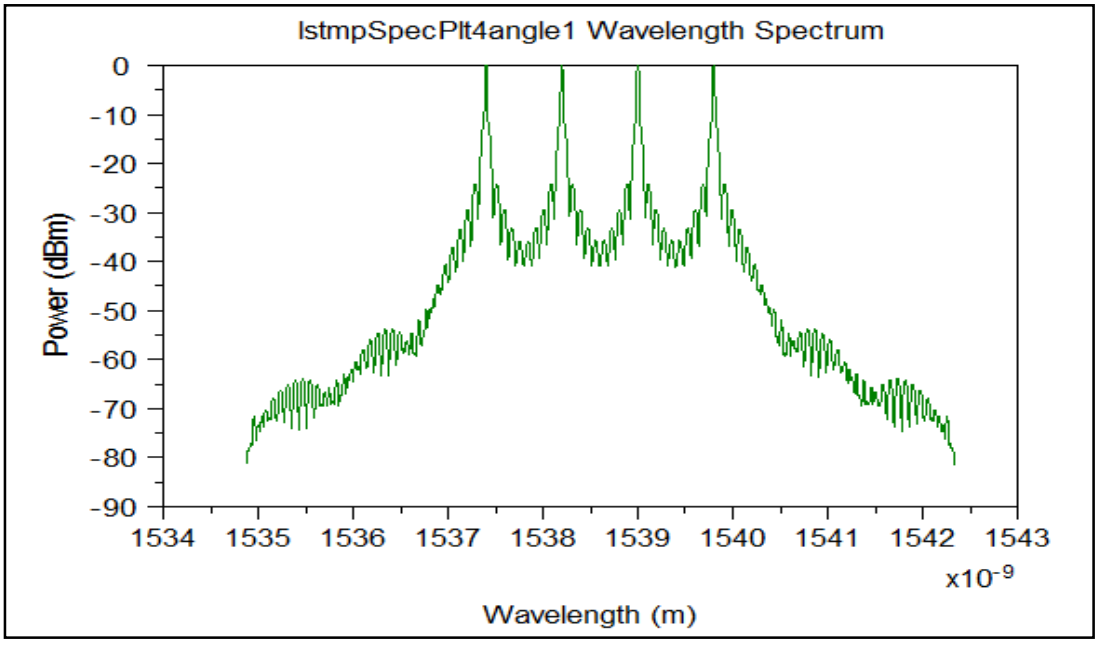

Fig 4.11 Wavelength spectrum for even channel

4.7 Combined Effect of polarisation at different length and angle of polarisation

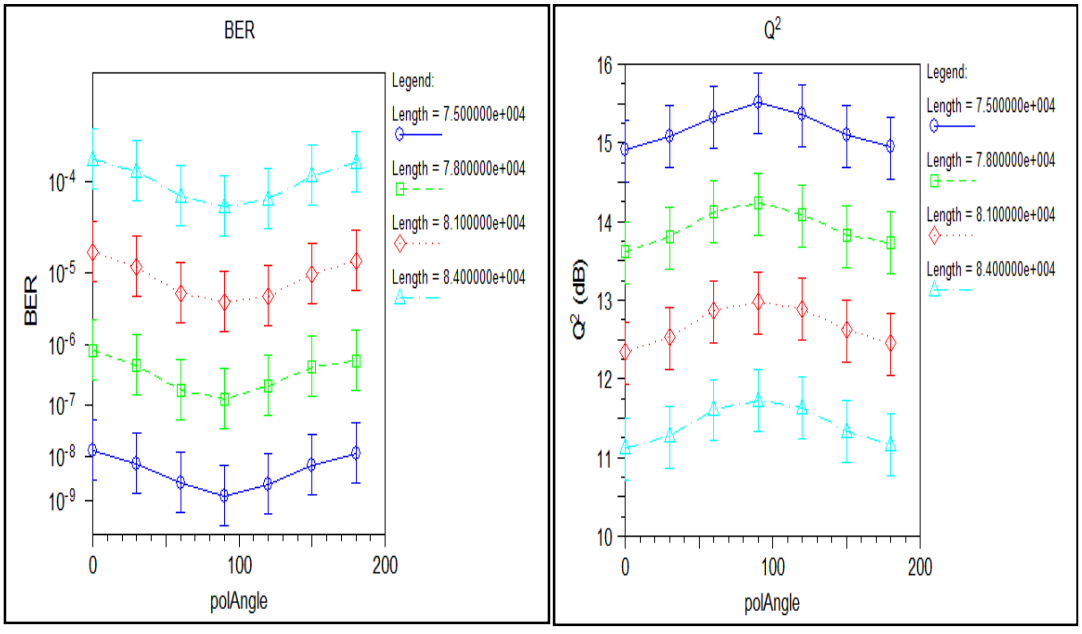

Fig.4.12 Combined effect of at variable length and polarization for odd channel

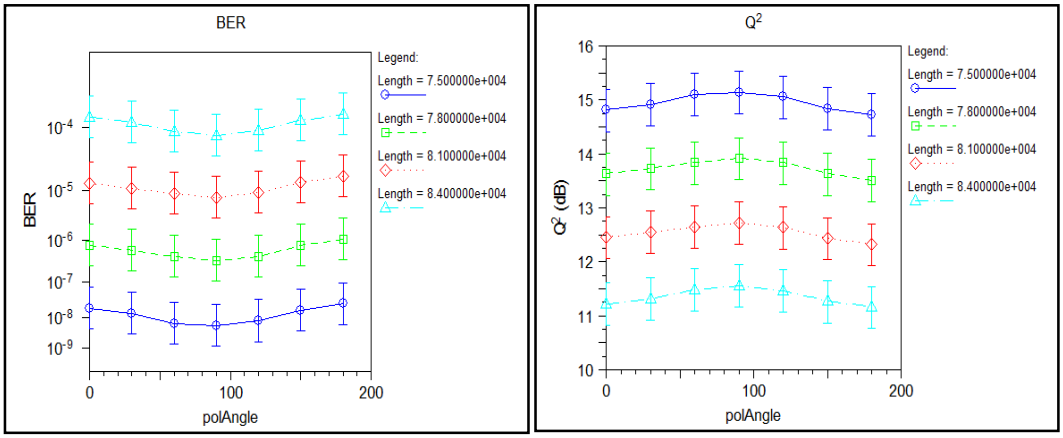

Fig. 4.13 Combined effect of at variable length and polarization for even channel

Table 4.1 Estimation of BER and Q-factor

Length of Fiber (in km)	Channel number	Polarization Angle					
		0 degree		90 degree		180 degree	
		BER	Q^2 dB	BER	Q^2 dB	BER	Q^2 dB
75	Channel 3	1.3359 x 10^{-8}	14.904	1.2304 x 10^{-9}	15.511	1.1593x 10^{-8}	14.943
	Channel 6	6.4175x 10^{-8}	14.455	5.1257x	15.158	1.3262x 10^{-7}	14.230
80	Channel 3	6.6343 x 10^{-6}	12.781	1.3934 x 10^{-6}	13.416	5.7718 x 10^{-6}	12.841
	Channel 6	6.6343 x 10^{-6}	12.781	13.934 x10^{-6}	13.416	5.7718 x 10^{-6}	12.841
85	Channel 3	3.0726 x 10^{-4}	10.694	1.0919 x 10^{-4}	11.356	2.9232 x 10^{-4}	10.728
	Channel 6	2.4081 x 10^{-4}	10.858	1.4209 x 10^{-4}	11.196	2.8713 x 10^{-4}	10.740

The above table represents BER and Q-factor observation at different length of fiber at even channel (un-polarized channel) and odd channel (polarized channels).

Chapter 5

CONCLUSION AND FUTURE ASPECTS

5.1 Conclusion

This chapter provides the summary of the research work done in this thesis. First the conclusion has been made from this study and then the suggestions for the future research are discussed. The major results obtained in this are summarized as follows:-

In this thesis, the scheme generating optical logic is implemented by MZ Interferometer as discussed in chapter 2. This scheme can easily and successfully be extended and implemented for any higher number of input digits by proper incorporation of MZI based optical switches, vertical and horizontal extension of the tree and by suitable branch selection. Again the whole operation is parallel in nature, i.e. the results of different operations between the data are obtained at a time. Here the multiple instruction multiple data type operation can be implemented nicely. Arithmetic operations can be conducted here between any two large-shaped data. The proposed one bit digital comparison scheme also successfully exploits non-linear material based tree structures for its operation. In order to experimentally achieve results from the proposed scheme, some design issues have to be considered. For example, walk-of problem due to dispersion, polarization properties of fiber, predetermined values of the intensities/wavelength of laser light for control and incoming signals, introduction of filter, intensity losses due to beam splitters/fiber couplers, etc. Practical implementation of the suggested scheme will be reported in future work. CW beam of wavelength 1535 nm and pulsed signal of wavelength 1500 nm can be used as incoming and control signals, respectively. Intensity losses due to beam splitters/couplers in the interconnecting stage may not create much trouble in producing the desired optical bits at the output as the whole system is a digital one and the output depends only on the presence or absence of light. In inter- connecting stages fiber-couplers can be used instead of beam splitters.

During the study of the polarization effect, it is demonstrated that various combinations of different polarization angles can be simulated efficiently and accurately to calculate BER and Q-factor. During this simulation, it is observed that at 90 degree polarization angle, minimum BER and maximum Q-factor can be achieved. If the effect of polarization is studied at different fiber lengths, as the length of fiber increases the BER also increases

but Q-factor decreases. This result holds that the polarization angle is independent of the length of fiber, i.e. for any length of fiber the effect of polarization is minimum at 90 degree. Using this, the receiver model can be improved using realistic filter shapes and to account for noise re-polarization during transmission.

5.2 Future Aspects

All-optical logic is recent research in the field of optical computing as this scheme also provides the idea of optical memory if an optical flip-flop is designed, which stores data as an optical pulse.

The field of optical wave division Multiplexing has experienced explosive growth over the past few years. As the WDM have many advantages over the all multiplexing techniques. This growth has been fuelled mainly by the demands for enormous bandwidth on our networks, namely the Internet, to satisfy the high applications of the network users. WDM has proven to be the current favourite technology for building optical network. The WDM advent of new information technology has created both opportunity and challenges. These opportunities and challenges are both economic and engineering in nature. Internet information travels through optical fibers. Today, optical fibers are being installed where a single fiber has the ability to carry information as much as 200 times faster than was possible just five years ago. This revolutionary capability is being achieved with technology known as wavelength division multiplexing WDM. WDM technology relies on the fact that optical fibers can carry many wavelengths of light simultaneously without interaction between each wavelength. Thus, a single fiber can carry many separate wavelength signals or channels simultaneously. The communications industry is at the onset of new expansion of WDM technology necessary to meet the new demand for bandwidth.

References:

[1] S. Bigo, A. Bertaina, et. al., "5.12 Tbit/s 128 _ 40 Gbit/s transmission over 3 _ 100 km of Teralight fiber," in *Proc. Eur. Conf. Optical Commun. (ECOC 2000)*, Munich, Germany, Sept. 2000.

[2] S. Kawanishi, et. al."3 Tbit/s (160 Gbit/s _ 19 channel) optical TDM and WDM transmission experiment," *Electron. Lett.*, vol. 35, no. 10, pp. 826–827, 1999.

[3] M. Nakazawa, et. al. "1.28 Tbit/s-70 km OTDM transmission using third and fourth-order simultaneous dispersion compensation with a phase modulator," *Electron. Lett.*, vol. 36, no. 24, pp. 2027–2029, 2000.

[4] K. Suzuki, K. Iwatsuki, S. Nishi, and M. Saruwatari, "Error-free demultiplexing of 160 Gbit/s pulse signal using loop mirror including semiconductor laser amplifier," *Electron. Lett.*, vol. 30, no. 18, pp. 1501–1503, 1994.

[5] K. L. Hall and B. S. Robinson, "Bit error characterization of 100 Gbit/s all-optical demultiplexers," in *Proc. Conf. Lasers and Electro-Optics* Baltimore, MD, 23–28, pp. 214–215, May *1999*,

[6] C. Schubert, et. al. "160-Gbit/s all-optical demultiplexing using a gain-transparent ultrafast-nonlinear interferometer (GT-Uni)," *IEEE Photon. Technol. Lett.*, vol. 13, pp. 475–477, May 2001.

[7] S. Nakamura, et.al. "Demultiplexing of 168-Gb/s data pulses with a hybrid-integrated symmetric Mach–Zehnder all-optical switch," *IEEE Photon. Technol. Lett.*, vol. 12, pp. 425–427, Apr. 2000.

[8] St. Fischer, et. al. "Ultrafast all-optical demultiplexer based on Mach–Zehnder interferometer with integrated semiconductor optical amplifiers," in *Proc. 5th Optoelectron. Commun. Conf. (OECC 2000)*, Chiba, Japan, pp. 566–567. July 2000

[9] S. Diez, R. Ludwig, and H. G. Weber, "Gain-transparent SOA-switch for high-bitrate OTDM add/drop multiplexing," *IEEE Photon. Technol. Lett.*, vol. 11, pp. 60–62, Jan. 1999. [10] M.T. Hill, et al., Coupled Mach–Zehnder interferometer memory element, Opt. Lett. 30 (13) (2005) 1710–1712.

[10] M.T. Hill, et al., Coupled Mach–Zehnder interferometer memory element, Opt. Lett. 30 (13) (2005) 1710–1712.

[11] S. Nakamura, Y. Ueno, K. Tajima, J. Sasaki, T. Sugimoto, T. Kato, T. Shimoda, M. Itoh, H. Hatakayama, T. Tamanuki, T. Sasaki, Demultiplexing of 168-Gb/s data pulses with a hybrid integrated symmetric Mach– Zehnder all-optical switch, IEEE Photon. Technol.

Lett. 12 (4) (2000) 425–427.

[12] St. Fischer, M. Dulk, M. Bitter, M. Caraccia, E. Gamper, E. Gini, W. Vogt, H. Melchior, W. Hunziker, A. Buxens, H.N. Paulsenand, A.T. Clausen, Ultrafast all-optical demultiplexer based on Mach–Zehnder interferometer with integrated semiconductor amplifiers, in: Proceedings of the Fifth Optoelectronic Communication Conference (OECC), Chiba, Japan, July 2000, pp. 566–567.

[13] R.P. Schreicek, M.H. Kwakernaak, H. Jackel, H. Melchior, All-optical switching at multi 100-Gb/sdata rates with Mach–Zehnder interferometer switches, IEEE J. Quantum Electron. 38 (8) (2002) 1053–1061.

[14] J. Leuthold, P.A. Besse, E. Gampber, M. Dulk, S. Fischer, G. Gueks, H. Melchior, All-optical Mach–Zehnder interferometer wavelength converters and switches with integrated data- and control-signal separation scheme, J. Lightwave Technol. 17 (1999) 1055–1066.

[15] M. Nakazawa, H. Kuboto, K. Suzuki, E. Yamada, A. Sahara, Ultrahigh-speed long-distance TDM and WDM soliton transmission technologies, IEEE J. Select. Top. Quantum Electron. 6 (2000) 363–396.

[16] S. Mukhopadhyay, An optical conversion system: from binary to decimal and decimal to binary, Opt. Commun. 76 (1990) 309–312.

[17] J.N. Roy, A.K. Maiti, S. Mukhopadhyay, Designing of an all-optical time division multiplexing scheme with the help of nonlinear material based tree-net architecture, Chin. Opt. Lett. 4 (8) (2006) 483–486.

[18] J. Nath Roy "Mach–Zehnder interferometer-based tree architecture for all-optical logic and arithmetic operations" 1 March 2007; accepted 10 September 2007

[19] M. Zhang, Ling Wang, and Peida Ye, Beijing "All-Optical Xor Logic Gates: Technologies And Experiment Demonstrations" IEEE Optical Communications May 2005

[20] T. Ivan Lima Efficient Computation of Outage Probabilities Due to Polarization Effects in a WDM System Using a Reduced Stokes Model and Importance Sampling IEEE photonics technology letters, vol. 15, no. 1, January 2003.

[21] P. J. Winzer, M. Pfennigbauer, M. M. Strasser, and W. R. Leeb, "Optimum filter bandwidth for optically preamplified NRZ receivers," *J. Lightwave Technol.*, vol. 19, pp. 1263–1273, Sept. 2001.

[22] S. J. Madden et. al."Four-Channel Polarization-Insensitive Optically Transparent Wavelength Converter" IEEE, vol. 9, no. 10, october 1997.

[23] M. Kovacevic and A. Acampora, "Benefits of wavelength translation in all-optical clear-channel networks," *IEEE J. Select. Areas Commun.,* vol. 14, pp. 868–880, May 1996.

[24] W. D. Zhong, J. P. R. Lacey, and R. S. Tucker, "Multiwavelength cross connects for optical transport networks," *J. Lightwave Technol.,* vol. 14, pp. 1613–1620, July 1996.

[25] N. Pleros "Optical signal processing using integrated multi-element SOA–MZI switch arrays for packet switching" IET Optoelectron., , 1, (3), pp. 120–126, June 2007

[26] G. Singh Design of 2x2 Optoelectronic Switch Based on MZI and Study the Effect of Electrode Switching Voltages vol. 29 MAY 2008